NAVAL POSTGRADUATE SCHOOL
Monterey, California

THESIS

EVALUATION OF ALTERNATIVE COMMUNICATION SCHEMES USING ENVIRONMENTALLY ADAPTIVE ALGORITHMS

by

Christos Athanasiou

June 2001

Thesis Advisors: Andrés Larraza
Kevin B. Smith
Monique P. Fargues

Approved for public release; distribution is unlimited

REPORT DOCUMENTATION PAGE			Form Approved OMB No. 0704-0188
Public reporting burden for this collection of information is estimated to average 1 hour per response, including the time for reviewing instruction, searching existing data sources, gathering and maintaining the data needed, and completing and reviewing the collection of information. Send comments regarding this burden estimate or any other aspect of this collection of information, including suggestions for reducing this burden, to Washington headquarters Services, Directorate for Information Operations and Reports, 1215 Jefferson Davis Highway, Suite 1204, Arlington, VA 22202-4302, and to the Office of Management and Budget, Paperwork Reduction Project (0704-0188) Washington DC 20503.			
1. AGENCY USE ONLY ***(Leave blank)***	**2. REPORT DATE** June 2001	**3. REPORT TYPE AND DATES COVERED** Master's Thesis	
4. TITLE AND SUBTITLE: Evaluation of Alternative Communication Schemes Using Environmentally Adaptive Algorithms			**5. FUNDING NUMBERS**
6. AUTHOR(S) Athanasiou, Christos			
7. PERFORMING ORGANIZATION NAME(S) AND ADDRESS(ES) Naval Postgraduate School Monterey, CA 93943-5000			**8. PERFORMING ORGANIZATION REPORT NUMBER**
9. SPONSORING / MONITORING AGENCY NAME(S) AND ADDRESS(ES) N/A			**10. SPONSORING / MONITORING AGENCY REPORT NUMBER**
11. SUPPLEMENTARY NOTES The views expressed in this thesis are those of the author and do not reflect the official policy or position of the Department of Defense or the U.S. Government.			
12a. DISTRIBUTION / AVAILABILITY STATEMENT Approved for for puplic release; distribution is unlimited.			**12b. DISTRIBUTION CODE**

13. ABSTRACT ***(maximum 200 words)***

Time-varying multipath propagation in a shallow underwater environment causes intersymbol interference in high-speed underwater acoustic (UWA) communications. Combating this effect is considered to be the most challenging task requiring large adaptive filters and increasing the computational burden at the receiver end.

This thesis presents results of an in-tank experiment and data analysis performed off-line to examine, evaluate, and compare the robustness of Time-Reversal Approach to Communications (TRAC) and the Matched Environment Signaling Scheme (MESS) in different conditions, such as noise, surface waves and range changes between the receiver and transmitter. Both methods examined can environmentally adapt the acoustic propagation effects of a UWA channel. The MESS method provides a communications solution with increased computational complexity at the receiver end but gives higher data rates and is more robust to the presence of noise, surface waves, and range changes than the TRAC method. On the other hand, the TRAC method manages to accomplish secure communications with low computational complexity at the receiver.

14. SUBJECT TERMS Matched enviroment signaling scheme, Time reversal acoustics, Acoustic communications, Acoustic signal processing, Acoustic telemetry			**15. NUMBER OF PAGES** 130
			16. PRICE CODE
17. SECURITY CLASSIFICATION OF REPORT Unclassified	**18. SECURITY CLASSIFICATION OF THIS PAGE** Unclassified	**19. SECURITY CLASSIFICATION OF ABSTRACT** Unclassified	**20. LIMITATION OF ABSTRACT** UL

NSN 7540-01-280-5500

Standard Form 298 (Rev. 2-89)
Prescribed by ANSI Std. 239-18

THIS PAGE INTENTIONALLY LEFT BLANK

Approved for public release; distribution is unlimited.

EVALUATION OF ALTERNATIVE COMMUNICATION SCHEMES USING ENVIRONMENTALLY ADAPTIVE ALGORITHMS

Christos Athanasiou
Lieutenant, Hellenic Navy
B.S., Hellenic Naval Academy, 1992

Submitted in partial fulfillment of the
requirements for the degrees of

MASTER OF SCIENCE IN ELECTRICAL ENGINEERING
and
MASTER OF SCIENCE IN APPLIED PHYSICS

from the

NAVAL POSTGRADUATE SCHOOL
June 2001

Author: _____
Christos Athanasiou

Approved by: _____
Andrés Larraza, Thesis Advisor

_____
Kevin B. Smith, Thesis Advisor

_____
Monique P. Fargues, Thesis Advisor

_____
William B. Maier, Chairman
Department of Physics

_____
J.B. Knorr, Chairman
Department of Electrical and Computer Engineering

THIS PAGE INTENTIONALLY LEFT BLANK

ABSTRACT

Time-varying multipath propagation in a shallow underwater environment causes intersymbol interference in high-speed underwater acoustic (UWA) communications. Combating this effect is considered to be the most challenging task requiring large adaptive filters and increasing the computational burden at the receiver end.

This thesis presents results of an in-tank experiment and data analysis performed off-line to examine, evaluate, and compare the robustness of Time-Reversal Approach to Communications (TRAC) and the Matched Environment Signaling Scheme (MESS) in different conditions, such as noise, surface waves and range changes between the receiver and transmitter. Both methods examined can environmentally adapt the acoustic propagation effects of a UWA channel. The MESS method provides a communications solution with increased computational complexity at the receiver end but gives higher data rates and is more robust to the presence of noise, surface waves, and range changes than the TRAC method. On the other hand, the TRAC method manages to accomplish secure communications with low computational complexity at the receiver.

THIS PAGE INTENTIONALLY LEFT BLANK

TABLE OF CONTENTS

THIS PAGE INTENTIONALLY LEFT BLANK

LIST OF FIGURES

THIS PAGE INTENTIONALLY LEFT BLANK

LIST OF TABLES

THIS PAGE INTENTIONALLY LEFT BLANK

EXECUTIVE SUMMARY

Sound propagation in an underwater communication channel becomes a very difficult task due to numerous constraints and limitations imposed by the nature of the medium and the environment. Available Signal-to-Noise Ratio is primarily limited by transmission loss and the presence of noise. Transmission loss, due to energy spreading and absorption, is increased with both frequency and range and limits severely the available bandwidth in a UWA communication channel. Noise presents strong frequency and site dependence and can become a very limiting factor in a shallow water environment. The most important characteristics of the underwater environment that put limitations on the Underwater Acoustic (UWA) communication systems' performance are the spatial and temporal variability and multipath propagation, which causes strong signal degradation.

In an UWA communication system, multipath propagation causes inter-symbol interference (ISI) and severe degradation of the acoustic communication signals. Fighting the effect of multipath propagation is considered to be the most challenging task in underwater acoustic communications.

The systems developed for UWA communications can be divided coarsely in two categories according to the performance limiting quantity, power or bandwidth. Power-limited UWA communication systems utilizing incoherent modulation schemes, such as Multiple Frequency Shift Keying (MFSK) systems, are appropriate to use, while in a bandwidth-limited environment coherent

systems using Differential Phase Shift Keying (DPSK) or Quadrature Amplitude Modulation (QAM) modulation techniques are the appropriate choice.

Incoherent systems utilize an energy-detection algorithm, which makes them reliable and inherently robust to time and frequency spreading. Nonetheless, in many non-coherent systems guard times are inserted between pulses of the same frequency to overcome the problem of multipath propagation. This leads to poor bandwidth efficiency (data rate/signal bandwidth) and low data rates. Up to now, none of the incoherent systems offer an *in situ* adaptation capability for determining channel reuse and setting the parameters of the system. As a result, these systems suffer from unnecessary bandwidth and power inefficiencies.

Coherent systems utilize a phase-detection algorithm allowing an efficient use of bandwidth and achieving high data rates at the same time. Depending on the method for carrier synchronization, phase-coherent systems are divided into two categories; differentially coherent and purely phase coherent. Phase-coherent signaling methods employ either some form of array processing, equalization methods, or a combination of both to compensate for the ISI. While bandwidth-efficient methods have been successfully tested in many types of channels, real-time systems have been implemented in short-range and vertical channels, where little multipath is observed and the phase stability is good.

A novel technique, called Time-Reversal Acoustics (TRA), has been developed to compensate for the difficulties encountered in UWA

communications using not a heavy computational algorithm in the receiver but the ocean itself as a matched filter for the acoustic propagation between the source and the receiver. This technique manages to focus the acoustic energy in space and in time at the receiver location eliminating any distortions introduced by the channel propagation. In a time-reversal acoustic system, the distorted received signal is recorded by an array and then transmitted back by co-located sources to the transmitter location in a time reversed fashion, meaning that the last signal received is first transmitted. As a result, all the modes arrive at the same time and add up constructively because the path back to the transmitter is reciprocally identical. It must be noted that in order to establish a communication link between the transmitter and the receiver, both participants must transmit in the medium (two-way communications).

Another communication technique, called Matched Environment Signaling Scheme (MESS), which is closely analogous to the TRA methods currently being investigated at NPS, was developed for the same purpose. This technique bears a heavier computational burden than the TRA technique because all the matched filtering is done in the receiver. However, this proposed matched filter technique is simpler to implement in the one-way transmission scheme.

The aim of the present thesis is to establish an experimental study for the evaluation of the best signal design for the MESS approach, examination and comparison of the robustness of the two communication schemes under different conditions. All the tests were performed in the Advanced Acoustic Research

Laboratory (AARL) and the processing of the data was done off-line using code developed in MATLAB.

Specifically, this experiment consists of supplying the basic set of four signals, which form 15 distinct symbols and a message containing all the symbols used. The bandwidth used in our tests for the signals is 50-65 kHz, which was found to be the best choice for our system. Subsequent analysis of the data recorded by the receiver under different conditions were performed offline by match-filtering the message with the received probe signals. The results from this analysis were compared with those using the Time Reversal Approach to Communications (TRAC).

We investigated the robustness of the MESS method with respect to time and under the influence of surface waves. Results show that correlation levels remain almost unchanged during the same day and decrease the following day with such rate that allows us to resolve a message using received probe signals captured the previous day. Results also indicate surface waves have little or no effect on correlation levels, allowing the message to be resolved without difficulty. However, the unaffected correlation due to surface waves can be explained by noticing that the waves were generated with conical pistons whose size is comparable with the wavelength of the waves, leading to cylindrical spreading and localized wave excitation regions. The scattering of sound by the rough surface and the Doppler effects were thus minimized, leaving the correlation level unaffected.

The computational load in the MESS method is very heavy, demanding fast processors and a large memory size due to the two correlation computations performed. Note that this load could be significantly decreased by using an FFT approach, where a power of 2 is selected in the computations. That is, compute the FFT of the message and the signals to be matched, multiply the first with the conjugate of the second, then compute the IFFT of the product.

The TRAC method has less computational complexity, as the underwater channel acts as the matched filter. However, the TRAC approach requires more power for transmission than the MESS approach, as all eight channels are used for transmission.

Experiments indicate that a symbol rate of 2500 symbols/sec is guaranteed for both methods when using a center-frequency spacing of 5 kHz, pulse length equal to 0.4 ms, Hanning window, and no inter-symbol spacing, which corresponds to a 10000 bits/sec data rate. These characteristics give us a spectral efficiency of (4 b/.4 ms)/25 kHz = 0.4 b/s/Hz for our basic signal. The MESS approach shows very low cross-talk amplitude between bits (frequencies), which ranges between ¼ - ½ of the cross-talk amplitude measured in the TRAC approach. Symbols resolution is improved and well-shaped pulses are created after processing the reception with the MESS approach. In addition, "peak splitting" using the TRAC method is very difficult to avoid, due to the sensitivity of the technique to the selection of the same time window for time-reversed signals.

We also investigated the ability of the MESS method to provide a higher data rate than the maximum rate the TRAC method provides, while keeping the cross-talk amplitude at less than the half of the maximum amplitude of the real peak. For this purpose, we decreased the pulse length to ~0.29 ms, which corresponded to a data rate of 14000 bits/sec. Experimental tests showed that it is feasible to achieve this data rate while maintaining the ability to resolve the message.

Experiments also show that the MESS approach is more robust in range changes than the TRAC approach. Specifically, we were able to resolve the message even 20 wavelengths away from the position where the replica of the transfer function of the channel was captured. The TRAC method proved to be very sensitive to range changes, as the absence of time focusing causes intersymbol interference outside the focal region. However, this sensitivity attributes a natural encryption to the message transmitted using the TRAC method for points outside the focal region.

Finally, we investigated the robustness of both methods in the presence of noise. For the evaluation of each scheme we computed the minimum SNR required for each center frequency in order for the message to be resolvable. The MESS approach displayed much better behavior in the presence of noise allowing us to resolve the message without errors for lower SNR's than the TRAC approach for all frequencies used. Specifically, using the MESS approach, we managed to resolve the message for SNR values approximately 1-10 dB less than those obtained by using the TRAC approach. The SNR improvement we get

using the MESS method can be attributed to the fact that not only the message but also the time-reversed signals, used for the message creation in the TRAC approach, already contain noise, since they are transmitted through the noisy channel. As a result, the noise power is much greater in the TRAC method than in the MESS approach.

THIS PAGE INTENTIONALLY LEFT BLANK

I. INTRODUCTION

Until recently, underwater acoustic (UWA) communication systems have been considered only in military applications. However, there is currently a growing interest in UWA communications for commercial applications. Some examples of non-military applications that have been developed during the last years include pollution monitoring, applications in the offshore industry, high quality video transmission from the bottom of the deep ocean, and scientific data collection without the need of retrieving the instruments. Also such systems have been employed in unmanned submersibles, such as robots and underwater vehicles, and nowadays there is an ongoing research for real-time communications with submarines and autonomous underwater vehicles not only in point-to-point links but also in networks configurations (Stojanovic, 1995 and Stojanovic, 1996).

Sound propagation in an underwater communication channel becomes a very difficult task due to numerous constraints and limitations imposed by the nature of the medium and the environment. Available Signal-to-Noise Ratio is primarily limited by transmission loss and the presence of noise. Transmission loss, due to energy spreading and absorption, is increased with both frequency and range and limits severely the available bandwidth in a UWA communication channel. Noise presents strong frequency and site dependence and can become a very limiting factor in a shallow water environment. The most important characteristics of the underwater environment that put limitations on the UWA

communication systems' performance are the spatial and temporal variability and multipath propagation, which causes strong signal degradation (Stojanovic, 1995 and Stojanovic, 1996).

Spatial variability is a result of the fact that the underwater channel acts as a waveguide, which causes various phenomena, such as the creation of shadow zones. This spatial variability can potentially cause severe problems, especially if the transmitter and the receiver are in relative motion.

In an UWA communication system, multipath propagation causes inter-symbol interference (ISI) and severe degradation of the acoustic communication signals. The mechanism that causes multipath propagation in shallow waters is primarily reflections at the surface and the bottom of the channel and at any object in the water. Fighting the effect of multipath propagation is considered to be the most challenging task in underwater acoustic communications.

The systems developed for UWA communications can be divided coarsely in two categories according to the performance limiting quantity, power or bandwidth. Power-limited UWA communication systems utilizing incoherent modulation schemes, such as Multiple Frequency Shift Keying (MFSK) systems, are appropriate to use, while in a bandwidth-limited environment coherent systems using Differential Phase Shift Keying (DPSK) or Quadrature Amplitude Modulation (QAM) modulation techniques are the appropriate choice (Kilfoyle et. al. 2000).

Incoherent systems utilize an energy-detection algorithm, which makes them reliable and inherently robust to time and frequency spreading.

Nonetheless, in many non-coherent systems guard times are inserted between pulses of the same frequency to overcome the problem of multipath propagation. This leads to poor bandwidth efficiency (data rate/signal bandwidth) and low data rates. Up to now, none of the incoherent systems offer an *in situ* adaptation capability for determining the rate with which the parameters of the system should be updated and adapted to new environmental conditions. As a result, these systems suffer from unnecessary bandwidth and power inefficiencies.

Coherent systems utilize a phase-detection algorithm allowing an efficient use of bandwidth and achieving high data rates at the same time. Depending on the method for carrier synchronization, phase-coherent systems are divided into two categories; differentially coherent and purely phase coherent. Phase-coherent signaling methods employ either some form of array processing, equalization methods, or a combination of both to compensate for the ISI. While bandwidth-efficient methods have been successfully tested in many types of channels, real-time systems have been implemented in short-range and vertical channels, where little multipath is observed and the phase stability is good (Stojanovic, 1996).

A novel technique, called Time-Reversal Acoustics (TRA), has been developed to compensate for the difficulties encountered in UWA communications using not a heavy computational algorithm in the receiver but the ocean itself as a matched filter for the acoustic propagation between the source and the receiver. This technique manages to focus the acoustic energy in space and in time at the receiver location eliminating any distortions introduced

by the channel propagation. In a time-reversal acoustic system, the distorted received signal is recorded by an array and then transmitted back by co-located sources to the transmitter location in a time reversed fashion, meaning that the last signal received is first transmitted. As a result, all the modes arrive at the same time and add up constructively because the path back to the transmitter is reciprocally identical. It must be noted that in order to establish a communication link between the transmitter and the receiver, both participants must transmit in the medium (two-way communications).

Another communication technique, which is closely analogous to the TRA methods currently being investigated at NPS, was developed for the same purpose. This technique bears a heavier computational burden than the TRA technique because all the matched filtering is done in the receiver. However, this proposed matched filter technique is simpler to implement in the one-way transmission scheme.

A non-coherent communication scheme using the TRA method was suggested by Abrantes et. al (1999) and Smith et. al (1999) and was established experimentally by Heinemann (2000). Non-coherent in this sense is meant to imply that no phase information was transmitted in the communication signal but instead an energy detector method was used.

In the tank tests performed in this thesis, a set of distinct signals representing binary bits is agreed upon and known by nodes **A** and **B**. Each signal sent from **A** should have roughly the same temporal resolution. A simple example would be multiple broadband signals with identical bandwidth, Hanning

window source spectra, and center frequencies separated by half the bandwidth (allowing for null detection between adjacent signals). The total number of signals within the set is then limited primarily by the bandwidth of the system. For example, four distinct signals (bits) within the set defining a 4-bit character will give values from 0-15, which is enough to build a full alpha-numeric code.

In the Time Reversal Approach to Communications (TRAC), the communications link is achieved when a single element of **A** transmits each signal to **B** with sufficient time between transmissions for all multipath structure to arrive. This provides **B** with the transfer function of the environment for those signals. Then **B** has the ability to transmit binary information to **A** by building 4-bit "symbols" out of the time-reversed signals. In addition, the transmission of subsequent symbols can overlap each other significantly. The criterion for the delay between subsequent symbol transmissions is the temporal resolution of the focus back at **A**. Furthermore, recall that these focused signals arriving back at **A** have an improved SNR. This scheme gives a high data rate system with the added benefits of longer range due to energy focusing and covert coding due to the inherent scrambling induced by the environment at points other than the intended receiver (Heinemann, 2000).

In the Matched Environment Signaling Scheme (MESS), the communications link is achieved when **A** transmits each basic signal to **B** with sufficient time between transmissions in order for station **B** to record the arrivals of the transmitted basic signal over all the distinct paths (multipaths). **B** then stores the arrivals of the primary signals in memory, which provides it with the

filters to use in subsequent messages. When a message is transmitted, **B** stores it into memory and then it match-filters it with the transfer function of the channel stored in the previous step.

The aim of the present thesis is to establish an experimental study for the evaluation of the best signal design for the MESS approach, examination and comparison of robustness of the MESS and TRAC communication schemes under different conditions. Specifically, this experiment consists of supplying the basic set of signals and a simple message. Subsequent analysis of the data recorded by **B** under different conditions will be performed offline by match-filtering the message with the primary signals. The results from this analysis will be compared with those using the TRAC scheme.

The remainder of this thesis consists of five chapters. Chapter II gives a brief overview of Time Reversal Acoustics theory and the necessary theoretical background for the MESS approach. Also, it provides the necessary formulation for the calculation of surface wave frequencies, created during our experiment in the tank to test the robustness of the MESS approach in a more complicated environment. In Chapter III we describe the tank, apparatus and software used in the tests. Chapter IV describes all tests and the data analysis performed off-line for the evaluation of the two methods. Chapter V presents the results for both methods examined. Finally, Chapter VI presents a comparative evaluation of the two methods investigated and identifies the points that require further research.

II. THEORETICAL BACKGROUND

This chapter presents an overview of time reversal acoustics theory and focuses particularly on pulse excitation because of its relevance with the experiments conducted using the Time Reversal Approach to Communications (TRAC). Also, we briefly present the necessary theoretical background behind the Matched Environment Signaling Scheme (MESS) and show its ability to increase the power of the received message by coherently adding the processed signal over all channels. Finally, we present the necessary formulation for the computation of the frequency of surface waves created to test the influence of a rough surface.

A. TIME REVERSAL ACOUSTICS THEORY

In this section we give a brief overview of the time reversal acoustics

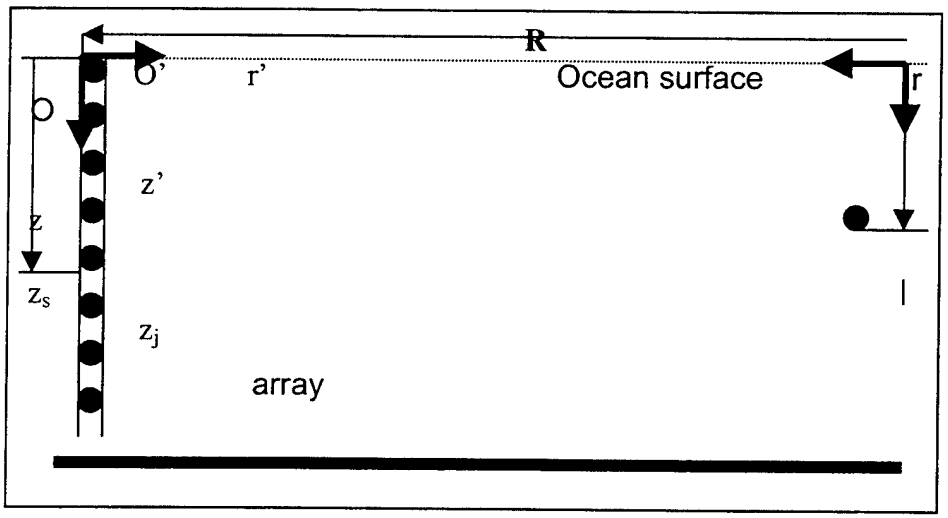

Figure 2.1. Geometry of the Experiment.

theory as described in Kuperman et al. (1998). Let's consider the waveguide of Fig. 2.1, which has a pressure release surface and rigid bottom. The reference

axis for propagation from the source and from the receiver are O and O', respectively. From Fig. 2.1 we can see that the coordinates are related by z'=z and r'=R-r, where R is the distance between the transmitter and receiver arrays. The point source is at range r=0 and lies at depth z_s. The j^{th} element of the receiving array, which consists of a total of J elements, is at depth z_j.

If the signal $s(t)$ is the initial pulse transmitted at frequency ω, the following time-domain signal is recorded by the j^{th} element of the receiver array:

$$p(R, z_j, t) = \int G(R, z_j \mid z_s, \omega) S(\omega) e^{-i\omega t} d\omega \,, \qquad (2.1)$$

where $S(\omega) = F[s(t)]$ is the Fourier transform of the initial signal $s(t)$. Here $p(R,z_j,t)$ is the pressure field as seen by the j^{th} array element at range R, depth z_j and time t. $G(R, z_j \mid z_s, \omega)$ denotes the frequency dependent Green's function in cylindrical coordinates at location (R,z_j) due to a point source at range r=0 and depth $z = z_s$. The Green's function represents the transfer function of the environment between source and receiver. This expression includes all effects of the waveguide environment, such as time elongation of the pulse due to multipath propagation. For convenience we set the time origin such that $P(R, z_j, t) = 0$ outside the time-interval $[0, \tau]$, where τ is large enough to include all the multipath arrivals. In order to maintain causality, the signal has to be completely received before it can be time reversed. So, the time-reversed signal that will be retransmitted from the j^{th} element will be $P(R, z_j, T-t)$, where T is such that $T > 2\tau$. Note that time reversal in the time-domain is the equivalent to

phase conjugation in the frequency-domain. The time-reversed signal can be written as

$$p(R, z_j, T-t) = \int G(R, z_j \mid z_s, \omega) S(\omega) e^{-i\omega(T-t)} d\omega \,. \tag{2.2}$$

If we use the conjugate symmetry property of the transmitted pulse, i.e., $S(-\omega) = S^*(\omega)$ and that of the Green's function, i.e., $G(R, z_j \mid z_s, -\omega) = G^*(R, z_j \mid z_s, \omega)$, and reverse the sign of the integration variable ω, Eq. (2.2) becomes

$$\begin{aligned} p(R, z_j, T-t) &= \int_{\infty}^{-\infty} G(R, z_j \mid z_s, -\omega) S(-\omega) e^{i\omega T} e^{-i\omega t} (-d\omega) \\ &= \int_{-\infty}^{\infty} [G^*(R, z_j \mid z_s, \omega) S^*(\omega) e^{i\omega T}] e^{-i\omega t} d\omega. \end{aligned} \tag{2.3}$$

The bracketed expression in Eq. (2.3) is the Fourier transform of the signal received by the j^{th} array element after time reversal and time-delay. Further, this expression is the frequency-domain representation of the retransmitted signal. From Eq. (2.3) we notice that the time reversal operation is equivalent to complex conjugation in the frequency domain plus a phase factor in order to retain causality.

Now, if the time-reversed signal is transmitted back to the source, the time reversed acoustic field generated by the j^{th} array element is given by

$$P_{TRA}(r', z \mid z_j, \omega) = G(r', z \mid z_j, \omega) G^*(R, z_j \mid z_s, \omega) S^*(\omega) e^{i\omega T}, \tag{2.4}$$

where $G\ (r^{'}, z\ |\ z_j, \omega)$ is the transfer function of the channel at location (r',z) due to a point source located at the j^{th} array element. The total field at location (r',z) is given by the superposition of the field generated by each individual array element, so

$$P_{TRA}(r^{'}, z \mid z_j, \omega) = \sum_{j=1}^{J} G\ (r^{'}, z\ \mid z_j, \omega) G^{*}(R, z_j \mid z_s, \omega) S^{*}(\omega) e^{i\omega T}\ . \qquad (2.5)$$

where J is the total number of array elements. The time domain representation of the pressure field is found by using Fourier synthesis, so that

$$p_{TRA}(r^{'}, z \mid z_j, t) = \sum_{j=1}^{J} \int G\ (r^{'}, z\ \mid z_j, \omega) G^{*}(R, z_j \mid z_s, \omega) S^{*}(\omega) e^{i\omega T} e^{-i\omega t} d\omega\ . \qquad (2.6)$$

Equation (2.6) can be used to show that the time reversal process produces focusing in time as well as in space back at the original source location. The temporal focusing can be displayed by examining the time-reversed field at the focus point, i.e., set $r = R,\ z = z_s$ in Eq. (2.6).

The reciprocity principle states that the acoustic field at $\vec{r_j}$ due to a point source located at $\vec{r_s}$ is equal to acoustic field that would be measured at $\vec{r_s}$ if the point source were located at $\vec{r_j}$ scaled by the ratio of densities at $\vec{r_s}$ and $\vec{r_j}$ (Jensen et al. (2000)). This can be formally written as

$$\rho(\vec{r_s}) G(\vec{r_j} \mid \vec{r_s}, \omega) = \rho(\vec{r_j}) G(\vec{r_s} \mid \vec{r_j}, \omega)\ . \qquad (2.7)$$

If we assume that the density is nearly constant throughout the channel and neglect the density gradients, reciprocity leads to $G(R,z_s \mid z_j,\omega) = G(R,z_j \mid z_s,\omega)$. The time-domain equivalent of Eq. (2.6) becomes (Kuperman et al. (1998))

$$p_{TRA}(R,z_s,t) = \frac{1}{(2\pi)^2}\left(\int \sum_{j=1}^{J} \left[\int g_{t'+t''}(R,z_s \mid z_j,\omega) g_{t'}(R,z_s \mid z_j,\omega) dt' \right] s(t''-t+T) \right) dt'' \quad , (2.8)$$

where $g_{t'+t''}(R,z_s \mid z_j,\omega), g_{t'}(R,z_s \mid z_j,\omega)$ and $s(t''-t+T)$ are the time-domain representations of the Green's function and the probe signal, respectively.

From Eq. (2.8) we notice that by implementing this method, the Green's function is correlated with itself, which corresponds to a matched filtering operation with the filter matched to the impulse response of the propagation from the source to the j^{th} array element. By autocorrelating the Green's function we succeed to compress the multipaths in time to the initial pulse length. The time elongation due to multipath propagation is reduced; hence, we produce focusing in time. The sum over all elements forms a spatial matched filter, so the signal focuses also in space.

B. MATCHED ENVIRONMENT TECHNIQUE

This technique is closely analogous to the TRA method but the matched filtering operation is not performed by the ocean but at the receiver itself. With this technique a probe signal is transmitted from the source before the message is released. The receiver array elements record the probe signal for a time-interval $[0,\tau]$, where τ is large enough to include all the multipath arrivals. In

the following we show how the matched filtering operation is performed and prove that the channels' receptions add coherently after performing the matched filtering.

1. Matched Environment Processing

Let's consider the transmitted probe signal p_{Pr}

$$p_{Pr}(0, z_s, t) = s_1(t), \tag{2.9}$$

and the transmitted message p_M, which is a combination of n different signals that make up a symbol transmitted at m various time symbols separated by T,

$$p_M(0, z_s, t) = \sum_m \sum_n a_{nm} s_n(t - mT), \tag{2.10}$$

where a_{nm} is the amplitude of the n^{th} signal in the m^{th} symbol.

The received signals are then

$$p_{Pr}(R, z_j, t) = G(R, z_j \mid z_s, t) \otimes s_1(t) + n_j(t), \tag{2.11}$$

and

$$p_M(R, z_j, t) = \sum_m \sum_n a_{nm} G(R, z_j \mid z_{s,}, t) \otimes s_n(t - mT) + n_j'(t), \tag{2.12}$$

where $\otimes$ represents the convolution operation, and $n_j(t)$ and $n_j'(t)$ represent additive noise contributions. The acoustic fields P_{Pr} and P_M generated by the probe signal and the message, respectively, are given in the frequency domain as the transform of Eq. (2.11) and Eq. (2.12),

$$P_{Pr}(R, z_j, \omega) = G(R, z_j \mid z_s, \omega) S_1(\omega) + N_j(\omega), \tag{2.13}$$

and

$$P_M(R, z_j, \omega) = \sum_m \sum_n a_{nm} G(R, z_j \mid z_{s,}, \omega) S_n(\omega) e^{-im\omega T} + N_j'(\omega) \quad (2.14)$$

Here we assume that the Green's function does not vary with respect to time, which is the case for a short period of time. If we correlate now $P_{\Pr}$ and P_M, we get in the frequency domain

$$S_{MESS}(R, z_j \mid z_s, \omega) = P_M(R, z_j \mid z_s, \omega) P_{pr}^*(R, z_j \mid z_s, \omega) =$$
$$\sum_m a_{1m} G(R, z_j \mid z_s, \omega) G^*(R, z_j \mid z_s, \omega) S_1^*(\omega) S_1(\omega) e^{-im\omega T} + A_j(\omega), \quad (2.15)$$

where $A_j(\omega)$ is defined as the incoherent cross-terms of the noise contribution at the element j. Note that the double summation of Eq. (2.14) reduces to a single summation in Eq. (2.15) because the received probe signal acts as a frequency domain filter that allows only $S_1(\omega)$ at its output.

The Inverse Fast Fourier Transform (IFFT) of Eq. (2.15) yields the lag domain representation of the processed signal, so

$$r_{MESS}(R, z_j, \tau) = \frac{1}{2\pi} \int G(R, z_j \mid z_s, \omega) G^*(R, z_j \mid z_s, \omega) S_1(\omega) S_1^*(\omega) \sum_m a_{1m} e^{i\omega(\tau - mT)} d\omega + \quad (2.16)$$
$$+ a_j(\tau).$$

Next, we define the signal **1** autocorrelation at element j as

$$X_{1j}(\tau) = \frac{1}{2\pi} \int G(R, z_j \mid z_s, \omega) G^*(R, z_j \mid z_s, \omega) S_1(\omega) S_1^*(\omega) e^{i\omega\tau} d\omega . \quad (2.17)$$

Then Eq. (2.16) can be written as

$$r_{MESS}(R,z_j,\tau) = \sum_m a_{1m} X_{1j}(\tau - mT) + a_j(\tau)\,. \qquad (2.18)$$

Because of the matched-filtering performed, Eq. (2.18) represents a series of autocorrelations of signal $s_1(t)$, which will peak at the zero lag times for each transmission m. We notice that by performing this matched-filtering operation we succeed to autocorrelate the Green's function, reducing in this way the multipath effects and compressing each processed symbol to the initial pulse length.

To reduce multipath effects further, we perform coherent addition of processed signals from each array element, which are now in phase due to the autocorrelations. The final processed message $R_{MESS}(R,\tau)$ with signal $s_1(t)$ is then

$$R_{MESS}(R,\tau) = \sum_j r_{MESS}(R,z_j,\tau) = \sum_m a_{1m} \sum_j X_{1j}(\tau - mT) + \sum_j a_j(\tau)\,. \qquad (2.19)$$

It should be noted that if we simply crosscorrelate the received message with the initial transmitted probe signal, the frequency domain representation of the processed message $S'_{XCORR}(R,z_j,\omega)$ is given by

$$S'_{XCORR}(R,z_j,\omega) = \sum_m a_{1m} G(R,z_j \mid z_s,\omega) S_1^{*}(\omega) S_1(\omega) e^{-im\omega T} + \\ + B_j(\omega), \qquad (2.20)$$

where $B_j(\omega)$ is defined as the noise contribution. The lag domain representation $r'_{XCORR}(R,z_j,\tau)$ of Eq. (2.20) would then be

$$r'_{XCORR}(R,z_j,\tau)=\frac{1}{2\pi}\int G(R,z_j \mid z_s,\omega)S_1(\omega)S_1^{*}(\omega)\sum_m a_{1m}e^{i\omega(\tau-mT)}d\omega + \\ +b_j(\tau). \tag{2.21}$$

From Eq. (2.21) it is obvious that by matched-filtering with the initial transmitted probe signal, the Green's function is not autocorrelated. As a result, the multipath effects are not removed and the processed message contains all the multipath arrivals, which can cause ISI. In addition, the channels cannot be added coherently.

C. SURFACE WAVE FREQUENCY CALCULATION

During our tests, it was necessary to investigate the robustness of the MESS approach to the presence of sea surface waves. For each frequency used in our experiment the frequency of the surface waves created was computed in such way that the wavelength of the acoustic and sea surface waves were equal. The formula used for this calculation is

$$\omega^2 = g\frac{2\pi}{\lambda}\tanh\left(\frac{2\pi h}{\lambda}\right), \tag{2.22}$$

where ω is the radial frequency of the surface waves, g is the acceleration of gravity, h is the depth of the acoustic channel, and λ is the wavelength of the acoustic wave. In our case, the quantity $(2\pi h/\lambda)>>1$, so $\tanh(2\pi h/\lambda)\approx 1$.

THIS PAGE INTENTIONALLY LEFT BLANK

III. APPARATUS DESCRIPTION AND EXPERIMENTAL SET-UP

In this chapter we describe briefly the apparatus used during our tests. A more thorough description has been given by Heinemann (2000). The experiment was conducted in the long tank located in the Advanced Acoustic Research Laboratory (AARL) at the Naval Postgraduate School. The main components of the set-up are the computerized data generation and acquisition system and the two transducer arrays.

A. THE TANK

The tank, shown in Fig. 3.1, is made of wooden plates and is covered with fiberglass for better sealing. Its inner dimensions are 15.32 m length, 1.17 m width and 1.20 m depth. The water depth is maintained at approximately 28 cm. Two rows of anechoic tiles, aligned vertically, cover the walls up to a height of 28 cm in order to reduce the echo reflection. Therefore, the tank acts as a horizontally infinite Pekeris waveguide with nearly rigid bottom and pressure release surface. The range to depth ratio of the water column is 54.71. As a result, the maximum range that can be considered is 10.94 km, if we assume that the tank simulates a shallow water environment of depth 200 m. In this experiment most of the tests were conducted in a distance of 5 m, which corresponds to a range of 3.6 km.

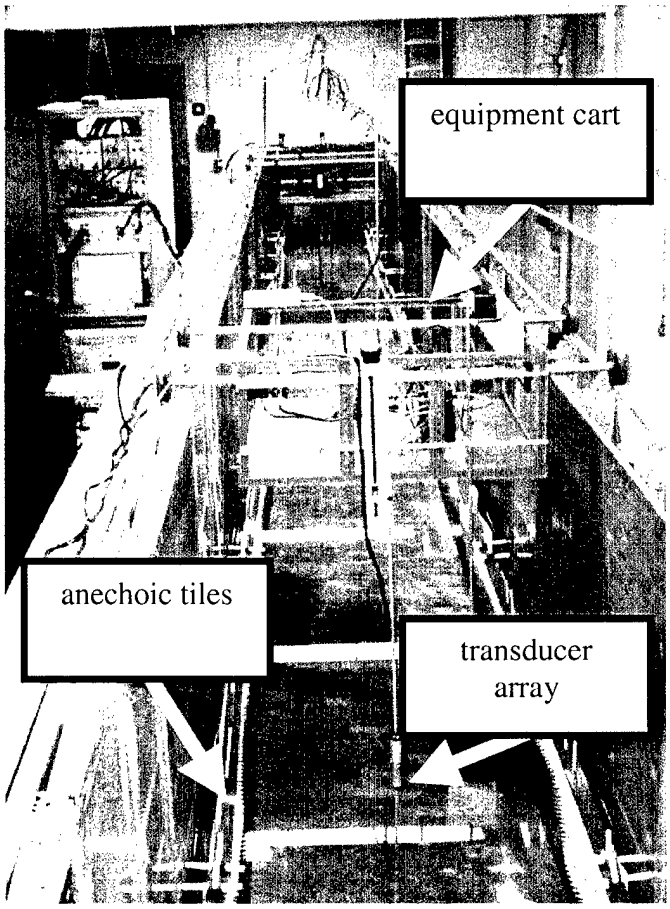

Figure 3.1. View from Above One End of the Tank. The tank has inner dimension of 15.32 m length, 1.17 m width and 1.20 m depth. The water level can be raised up to 28cm, the height of the anechoic material (From Heinemann, 2000).

On the top of the tank, a rail system facilitates the movement of two carts, which carry the transducers and the related computer controlled motors.

B. APPARATUS

1. The Transducers Arrays

Each transducer array consists of 10 cylindrical, horizontally omni-directional piezo-ceramic elements. The resonance frequency of the elements is 73 kHz. The elements are arranged vertically in a PVC tube. The dimensions of the arrays are shown in Fig. 3.2. Only elements 2 to 10 were used throughout our tests.

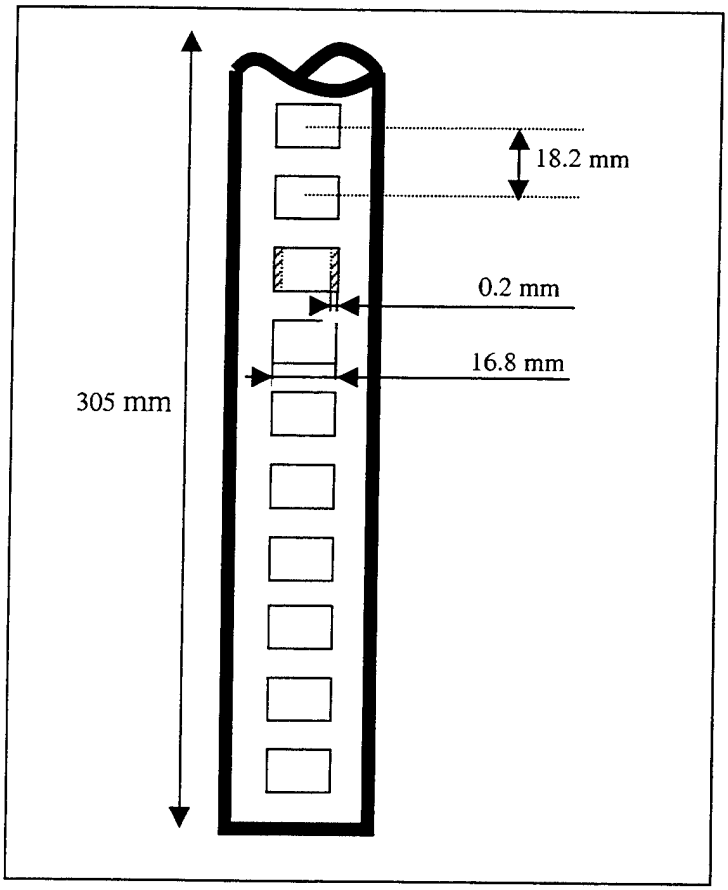

Figure 3.2. The Design of the Ten-Element Transducer Array. The arrays were made by EDO Electro-Ceramic Products and have dimensions 38 mm in diameter and 305 mm in length (From Heinemann, 2000).

2. The Computerized Signal Generation and Data Acquisition System

The data acquisition and generation system is a PC-based system developed by Gage Applied Sciences, Inc. It consists of a computer with a 200 MHz Pentium II CPU, eight CompuGen 1100 function generator cards and four dual channel CompuScope 512 oscilloscope cards. These cards provide us with a total of eight input and eight output channels.

3. Amplifiers

A set of eight HP 467A amplifiers was used for the amplification of the output of the signal generation cards. The maximum output of each amplifier was measured and found to be about 28 V.

4. Preamplifiers

A set of eight Stanford SR560 preamplifiers was used for the pre-amplification of the received signals before they are captured by the oscilloscope. Also, a built-in filter filters all the receptions allowing signals only in the band 10-300 kHz.

5. Switch

An eight-relay switch arrangement is used to interchange the role of the two transducer arrays as transmitter and receiver. It switches the connections from the amplifier and preamplifier banks to the transducer arrays 1 and 2.

6. Remote Control Equipment

The position of one of the carts can be changed in range remotely from the computer system using a radio transmitter set and stepping motors. Also, the height of the two-transducer arrays may be changed in the same way.

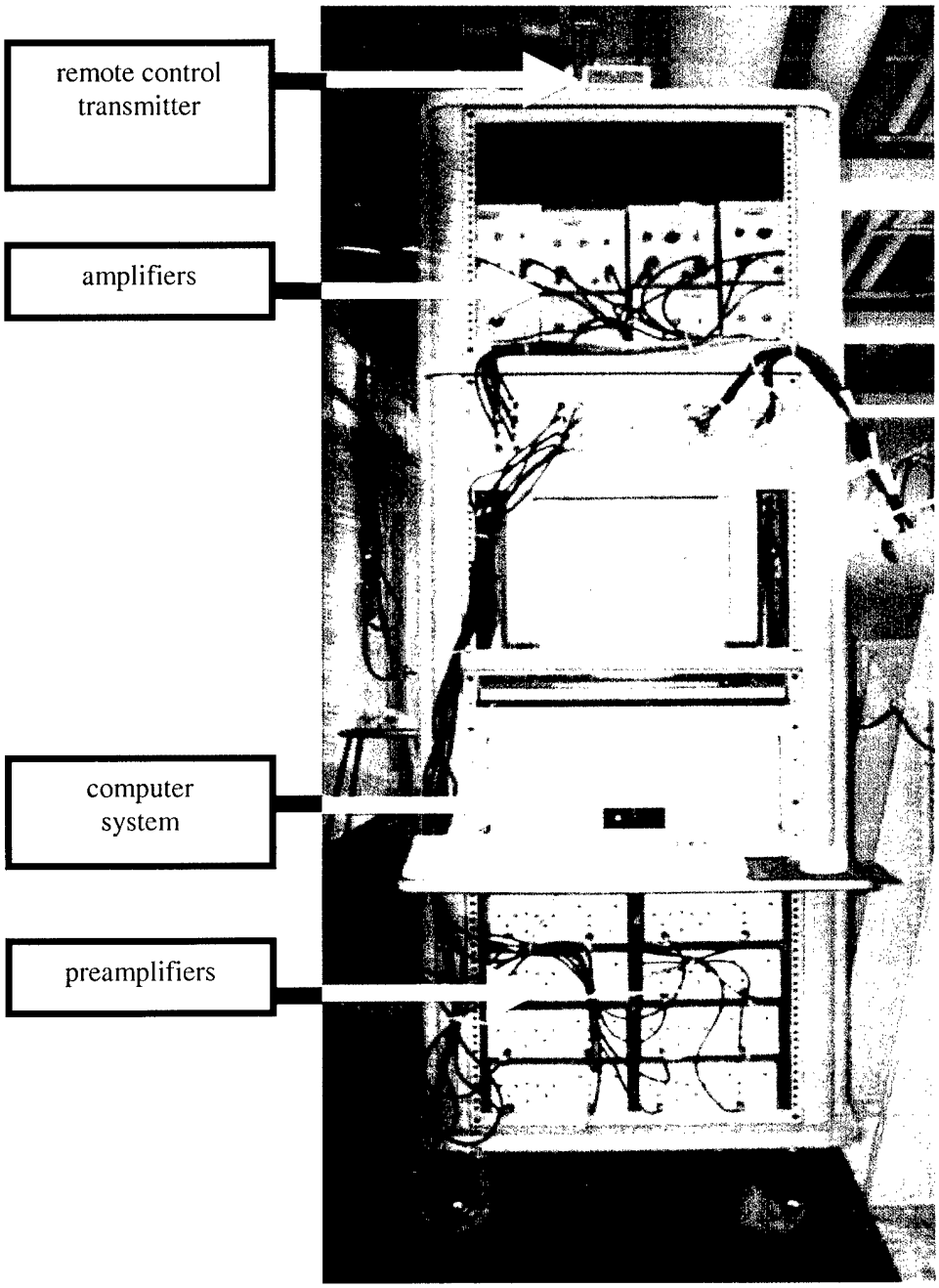

Figure 3.3. The Computer System with the Preamplifiers, the 8-Channel-Switch, the Amplifiers and Remote Control Transmitter (From Heinemann, 2000).

7. Wave Generation Equipment

Two conical pistons connected to matching speakers through rods were used to generate surface waves. The effective diameter of the cones is about 5 cm, and the excursion amplitudes are about 5 mm. The amplified output of an HP 8904A dual channel multifunction synthesizer connected to a TECHRON 5507 power amplifier was used to drive the speakers, so that the relative phase of the speakers can be controlled.

8. Noise Generation Equipment

A 1390-B noise generator connected to a 3988 low-pass/high-pass Butterworth-Bessel dual channel filter and a HP 467A amplifier was used for the noise influence tests. The settings of the filter allowed noise to be transmitted only in the band of 40-75 kHz.

C. SOFTWARE

MATLAB software, written by Michael Heinemann, was used for all the transmissions and data acquisition. In some cases, the code was modified to meet our needs. Also, a separate program was written by the author and used to process all the data off-line. Among the key features are editing of captured and processed signals, data storing, visualization and analysis of the data using both methods examined. Finally, a separate code was developed for the temporal coherence and wave influence tests and for the computation of the SNR level.

IV. EXPERIMENT DESCRIPTION

In this chapter we describe the experiments we conducted using the Matched Environment Signaling Scheme (MESS) and the Time Reversal Approach To Communications (TRAC).

The distance between the transducer arrays throughout the experiment was in most cases 5 m. The sampling rate used in all cases was 5 Msamples/sec. The frequency range used throughout the experiment is between 50 kHz and 65 kHz, which was found to be the best choice for our system (Heinemman, 2000). This frequency range was equally divided with a fixed frequency spacing of 5 kHz, and four center frequencies at 50 kHz, 55 kHz, 60 kHz and 65 kHz.

A. DEFINITION OF SYMBOLS

In the above mentioned communication schemes we used symbols that consist of four bits, each on a different frequency. The value of a bit is determined by the presence or absence of a pulse at the frequency assigned to that bit. The pulses at the different frequencies (bit values) are transmitted simultaneously. A set of four simultaneous pulses centered at four different frequencies constitutes a symbol (pulses may be absent at some frequencies if bit value is zero). These symbols contain information that can be related to a code. The number of symbols that can be produced using the above four frequencies is fifteen if we exclude the case that no frequency is selected (no

acoustic energy contained). For each symbol a number is assigned, as shown in Table 4.1.

SYMBOL NUMBER	S0	S1	S2	S3	S4	S5	S6	S7	S8	S9	S10	S11	S12	S13	S14
Center-Freq. 1	X		x		x		x		X		x		x		x
Center-Freq. 2		x	x			x	x			x	x			x	x
Center-Freq. 3				x	x	x	x					X	x	x	x
Center-Freq. 4								X	X	x	x	X	x	x	x

Table 4.1. Symbol Definition Table (After Heinemman, 2000).

Using the above symbols, we can create a simple alphanumeric code shown in Table 4.2 (Heinemman, 2000) or we can map the symbols to four-bit sequences for binary data transfer through an underwater channel or even establish a voice communications scheme using LPC-10 (2.4 kb/sec) U.S. standard.

General	
Symbol	**Meaning**
14	number follows
15	word follows
(space)	shift for second half of letters

Numbers	
Symbol	**Meaning**
1	1
2	2
3	3
4	4
5	5
6	6
7	7
8	8
9	9
10	0
11	+
12	-
13	.

Letters	
Symbol	**Meaning**
1	A
2	B
3	C
4	D
5	E
6	F
7	G
8	H
9	I
10	J
11	K
12	L
13	M
1	N
2	O
3	P
4	Q
5	R
6	S
7	T
8	U
9	V
10	W
11	X
12	Y
13	Z

Table 4.2 Simple Code Using 15 Symbols (From Heinemman, 2000).

B. RESOLUTION OF SYMBOLS

We will refer to signal A, B, C, and D as those pulses which contain only one of the above center frequencies, respectively. Each symbol has a time length of 0.4 ms and a Hanning window envelope. This pulse width corresponds to a null-to-null bit bandwidth of 10 kHz and a null-to-null symbol bandwidth of 25 kHz (for a symbol that contains all four center frequencies). The 0.4 ms Hanning window and its spectrum is shown in Fig. 4.1a and Fig.4.1b respectively. These features of the symbols are followed throughout the experiment unless otherwise noted. Also, a symbol containing all four frequencies and its spectrum is shown in Fig. 4.2a and Fig. 4.2b, respectively.

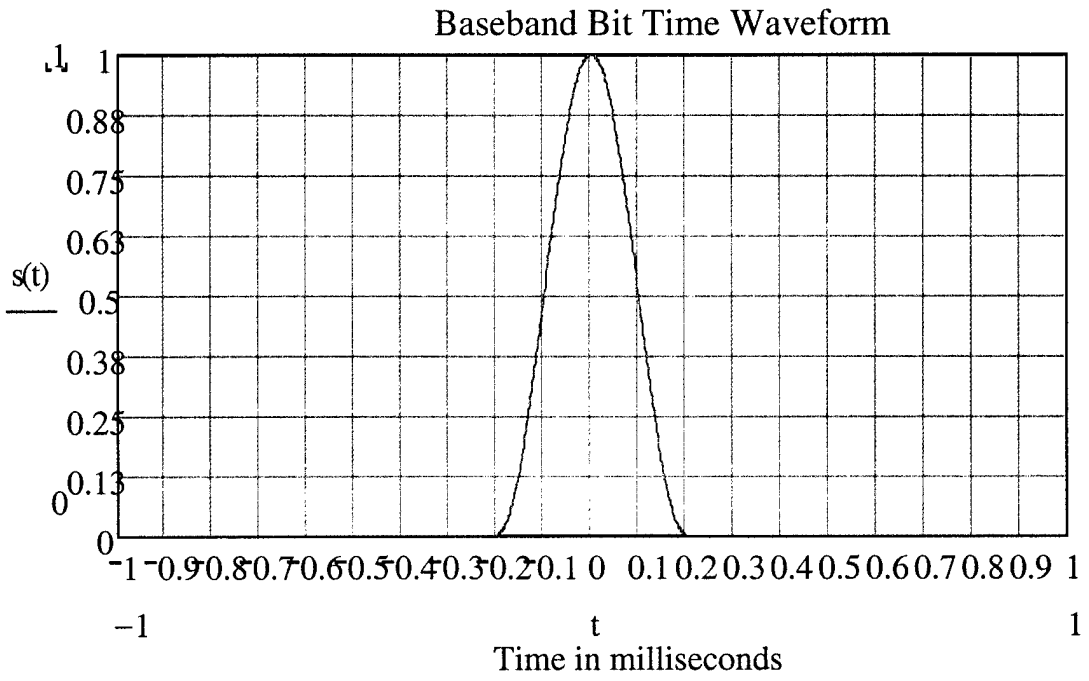

Figure 4.1a. Hanning Window of 0.4 ms Duration.

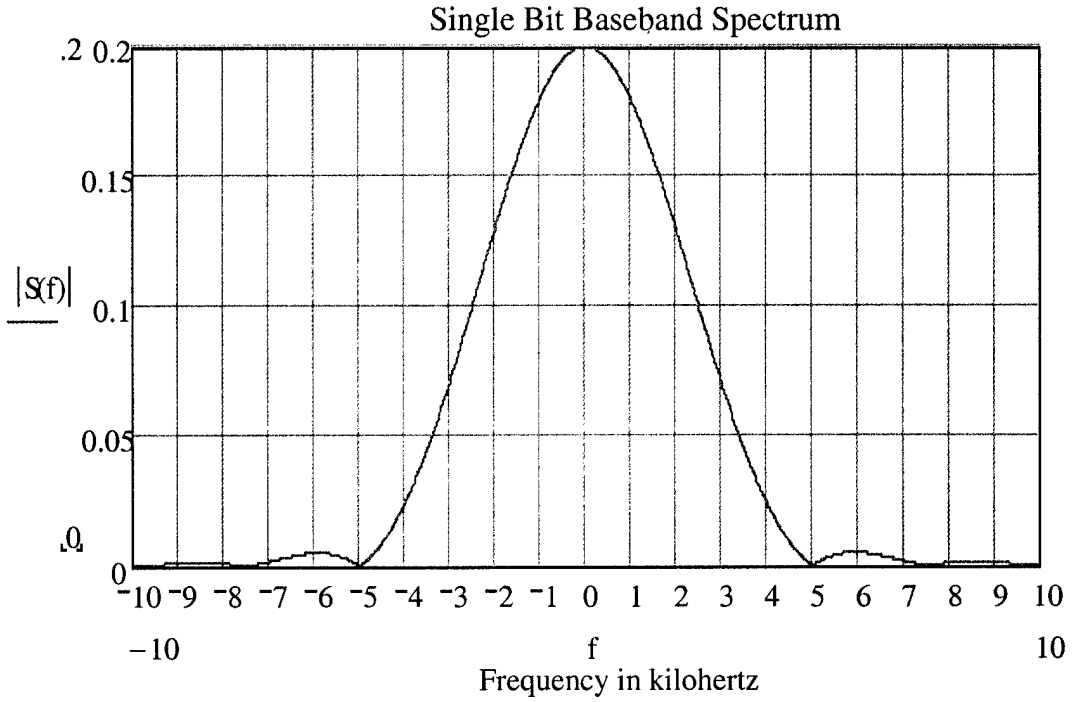

Figure 4.1b. Spectrum of a 0.4 ms Hanning Window.

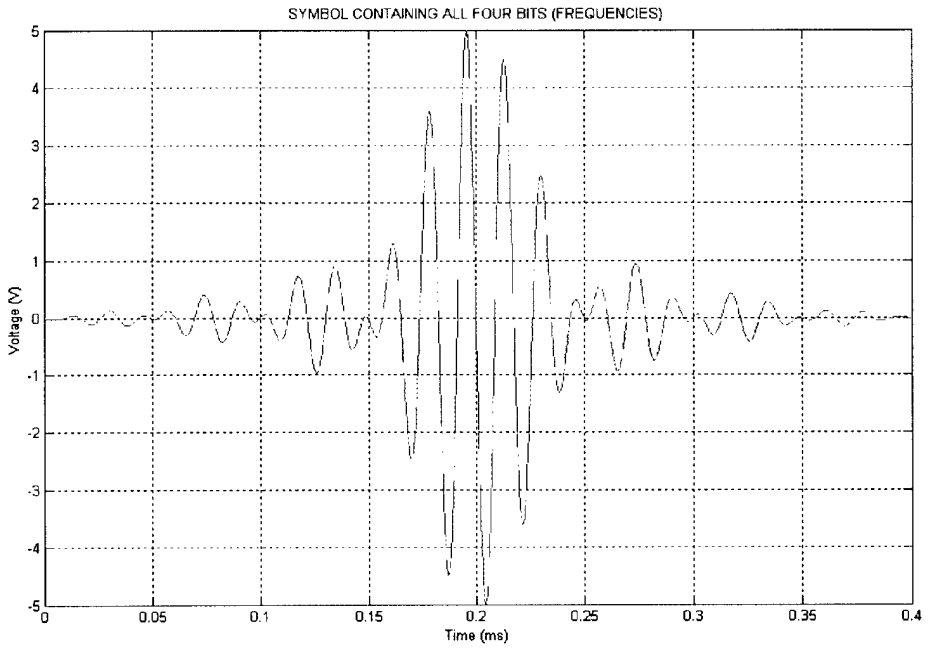

Figure 4.2a. Symbol Containing All Four Frequencies.

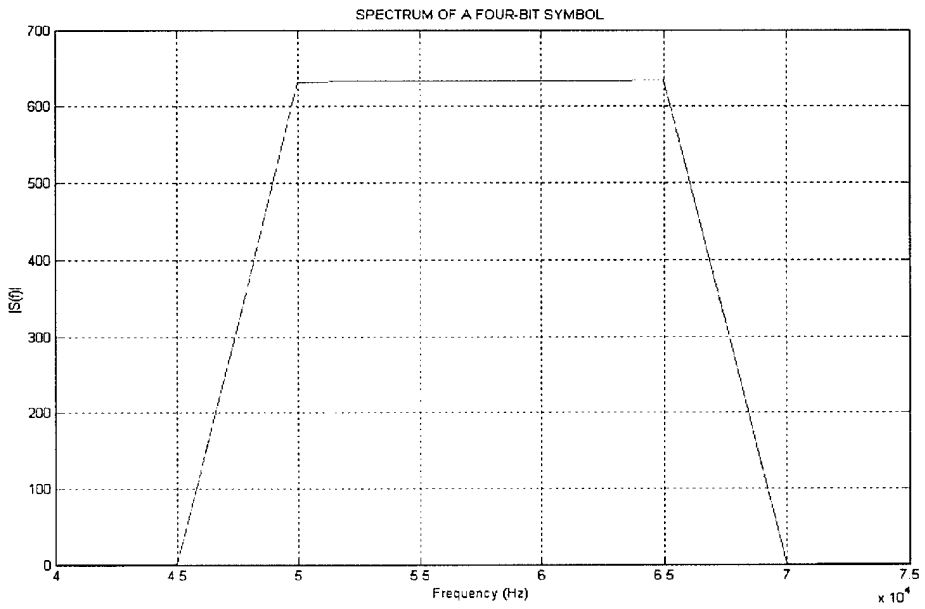

Figure 4.2b. Spectrum of a 4-bit symbol.

C. BANDWIDTH AND SPACING BETWEEN SYMBOLS

Besides using a bit bandwidth of 10 kHz for each symbol, we examined the resolvability of the message by using a bit bandwidth of 14 kHz and varying the spacing between symbols from 0 to 10 ms.

D. PROCEDURE DESCRIPTION

We sent messages and checked whether we could resolve them qualitatively without any errors by a matched filter approach for both signaling schemes.

1. Matched Environment Signal Processing

We wish to transmit information from position T (the transmitter position) to position R (the receiver position). Our communications approach is then based on matched-filtering the messages transmitted from T to R with replicas of

the transfer functions for the specific frequencies used, based on initialization of the signaling scheme.

Specifically, the transmissions were done with element #6 (channel #4) of transducer array #1 used as a transmitter and elements 2 to 10 (channels #1 through #8) of transducer array #2 as a receiver. The processing described below was performed for every channel of the receiver. A sequence of signals A, B, C, and D with predetermined spacing was transmitted either before the message or as the first part of the message. After performing several tests to determine the approximate response of the channel for each frequency, we adjusted the relative amplitudes of the center-frequencies in each symbol while keeping them constant for every symbol. This adjustment was necessary in order to keep the correlation level for a specific center frequency constant for every symbol as well as to keep the total output voltage of the amplifiers within their operating limitations. The resulting reception contained all the multipath propagation. The received sequence was match-filtered with signals A, B, C, and D. We then cut the match-filtered reception into 4 signals, which from now on will be referred to as prototypes. In other words each prototype contains the response of the channel for the corresponding signal. The time length of each prototype is equal to the pulse transmission interval of the initial sequence (pulse length + spacing). Then the messages were transmitted, which in most cases contained all 15 symbols. The received message was first match-filtered with signals A, B, C, and D and the resulting files were then match-filtered with the corresponding prototypes. After doing the processing for all the channels, we

coherently summed the processed data across the channels. A block diagram of the process described above is shown in Fig. 4.3.

2. Time Reversal Signal Processing

We wish to transmit information from position T (the transmitter) to position R (the receiver). As a first step, initial signals are transmitted from R to T and their receptions are time-reversed. TRAC approach is then based on the concept that the underwater channel acts as the matched filter of the time-reversed signal.

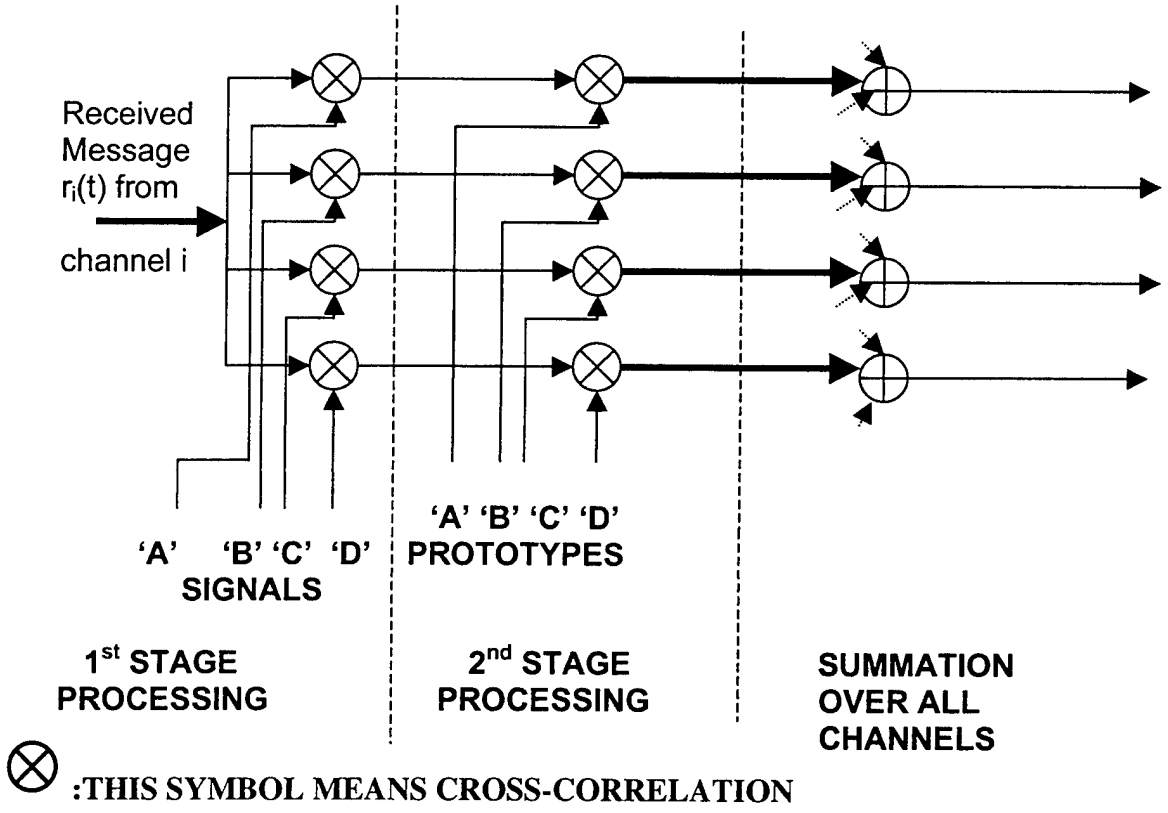

Figure 4.3. Block Diagram of the MESS Processing Scheme.

In more detail, the transmissions of the signals A, B, C, and D were done in most cases with element #6 (channel #4) of transducer array #1 used as a

transmitter and elements 2 to 10 (channels #1 through #8) of transducer array #2 as a receiver. Signals A, B, C, and D were transmitted separately before the message. The resulting reception has predetermined length and contains all the multipath propagation information. Then the 4 receptions were time-reversed in order to create the time-reversed signals. These signals are used to build the messages containing the above 15 symbols. The spacing between the symbols varied from none to 2 ms. We used the knowledge of the response of the channel for each frequency to adjust the relative amplitudes of the center-frequencies in each symbol while keeping them constant for every symbol. The above procedure was followed for all the channels of the receiver. The transmission of the message was done with elements 2 to 10 (channels #1 through #8) of transducer array #2 used as a transmitter and elements 2 to 10 (channels #1 through #8) of transducer array #1 as a receiver. Finally, the reception from channel #4, where the temporal and spatial focus was supposed to occur, was match-filtered with signals A, B, C, and D.

E. TEMPORAL COHERENCE TEST

We first examined the temporal coherence of the tank in order to find the associated decorrelation time for the four signals A, B, C, and D. For this purpose, four signal sequences were created. The duration of each sequence is 40.4 ms and the sequence timing description is shown in Table 4.3.

SEQUENCE TIMING DESCRIPTION					
SEQUENCE	0.0 sec	0.01 sec	0.02 sec	0.03 sec	0.04 sec
S1	A	A	A	A	A
S2	B	B	B	B	B
S3	C	C	C	C	C
S4	D	D	D	D	D

Table 4.3. Sequence Timing Description Table.

For each sequence a transmission schedule of one-hour duration was created. During the first ten minutes the sequence was transmitted every two minutes and after that we had a transmission every ten minutes. The same transmission schedule was also followed the next day. Performing this procedure, allowed us to determine the rate with which the correlation level decreased in the tank for each center frequency.

Each reception was matched-filtered with the corresponding signals A, B, C, and D on all channels. The matched-filtered receptions were then cut into chunks of 10 ms. The first chunk of each transmission schedule (for both days) was used as a prototype and was matched-filtered with the corresponding chunks. Finally, we coherently summed across channels for the chunks and observed the correlation level.

F. WAVE INFLUENCE

We examined the behavior of the underwater channel for the four frequencies used under the presence of waves. For this purpose the correlation level was measured by implementing the same procedure as that used in the temporal coherence test. However, now the measurements and processing were

performed for the cases of wave presence and absence. In order to create waves in the tank, the wave generators described in Chapter III were used with excitation frequencies calculated using Eq.(2.22) in Chapter II. Each time waves were created with wavelength equal to the wavelength of the acoustic pulse transmitted.

G. SYMBOL RATE TEST

To determine the maximum symbol rate that allows us to resolve the message, we changed the following three parameters of the transmission: the transmission interval, the received probe signal record length, and the pulse length. The criterion that determines the resolvability of a message is that the cross-talk amplitude between bits (frequencies), after the processing of the reception, should be less than half the amplitude of the peak values of existing pulses after performing proccessing.

1. Symbol Transmission Interval

We varied the symbol spacing of the transmission in order to investigate the minimum allowable spacing necessary to resolve the message. In our test we considered spacing of 10, 5, 2, 1, and 0 ms.

2. Received Probe Signal Record Length

For a symbol rate of 2500 symbols per second we investigated the role that the length of the received probe signal plays in the resolvability of the message using the matched environment technique. For this purpose, we matched-filtered the received message with probe signals of duration 2, 1, and 0.4 ms.

3. Pulse Length

For the matched environment approach, we examined the possibility of a higher symbol rate by changing the pulse to ~0.29 ms, corresponding to a symbol bandwidth of 14 kHz.

H. RANGE DEPENDENCY

We examined the resolvability of the message for different ranges using the prototype signals captured at the range of 4 m, by varying the distance between the transducers in steps of ±10 cm. The measurements took place over the range of 3.5 to 4.5 m. In addition, measurements were also performed at a distance of 5 m over the range of 4.5 to 5.5 m to verify the results. The same procedure was followed for the TRAC technique with the time-reversed signals captured at 4 m.

I. INFLUENCE OF THE NOISE

We investigated the robustness of both methods in noisy environment conditions. For this purpose, we created white noise, filtered it in the band of 40-75 kHz in order to cover all the bandwidth used in our signals, and transmitted it into the tank using a projector. Then, we determined the minimum SNR for each bit (center frequency) at the input of the receiver for which the message is still resolvable. For this purpose, we increased gradually the noise level in the tank and transmitted the message. For the creation of both prototype and time-reversed signals the initial signals A, B, C, and D were transmitted in the presence of noise with the same noise level used during the message transmission. Finally, we retransmitted the time-reversed signals in the presence of the same noise level.

For the computation of the SNR for each of the signals, we filtered the first reception of the initial signals for all eight channels and the second reception of the time-reversed signals for channel #4 using a high-order FIR filter over four different bands. The bands used here are 45 kHz-55 kHz, 50 kHz-60 kHz, 55 kHz-65 kHz, and 60 kHz-70 kHz. We also filtered the part of each received message where only noise is present with the same filters as above. Next, we computed the power spectral density of the filtered receptions over the different bands and calculated the SNR for each signal.

V. DATA ANALYSIS AND RESULTS

In this chapter we describe and evaluate the results of the experiments conducted using the procedures described in Chapter IV.

A. TEMPORAL COHERENCE TEST

It is very important for the correct evaluation of the experimental results to determine the time period after which we should retransmit signals A, B, C, and D in order to create new prototypes for the match-filtering procedure. In other words, we should determine the rate with which the response of the channel changes in time for the frequencies used. This time will be referred to as the decorrelation time.

For this purpose the correlation level was measured for each transmitted pulse after the processing was conducted, as described in Chapter IV. The results are presented in Fig. 5.1a through Fig. 5.1d for each of the frequencies used and for both days. It should be noted that the 'Transmission Number' in the plots does not relate linearly with time.

We notice that the correlation level remains almost steady during the same day for all the frequencies examined. The rate with which the correlation level decreases is approximately 3% for signal A, 12% for signal B, and 6% for signals C, D. As a result it can be considered safe to keep the same prototype throughout the same day and acceptable to be used for the next day. For validation of the above observation a message was transmitted and the reception

was match-filtered with prototypes captured the previous day. The results are shown in Fig. 5.2. We notice that the message is easily resolvable.

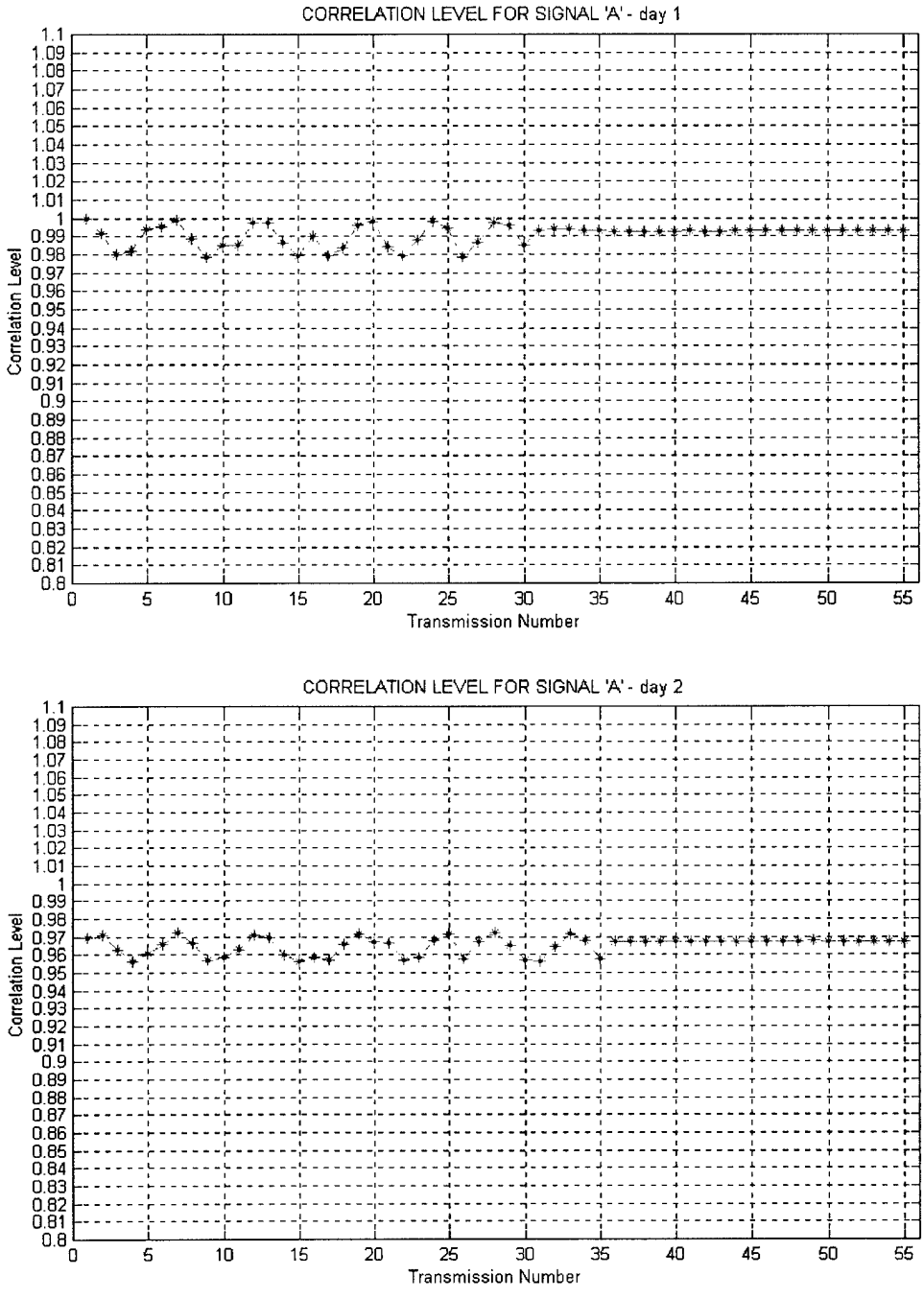

Figure 5.1a. Correlation Level for Signal A (Both days).

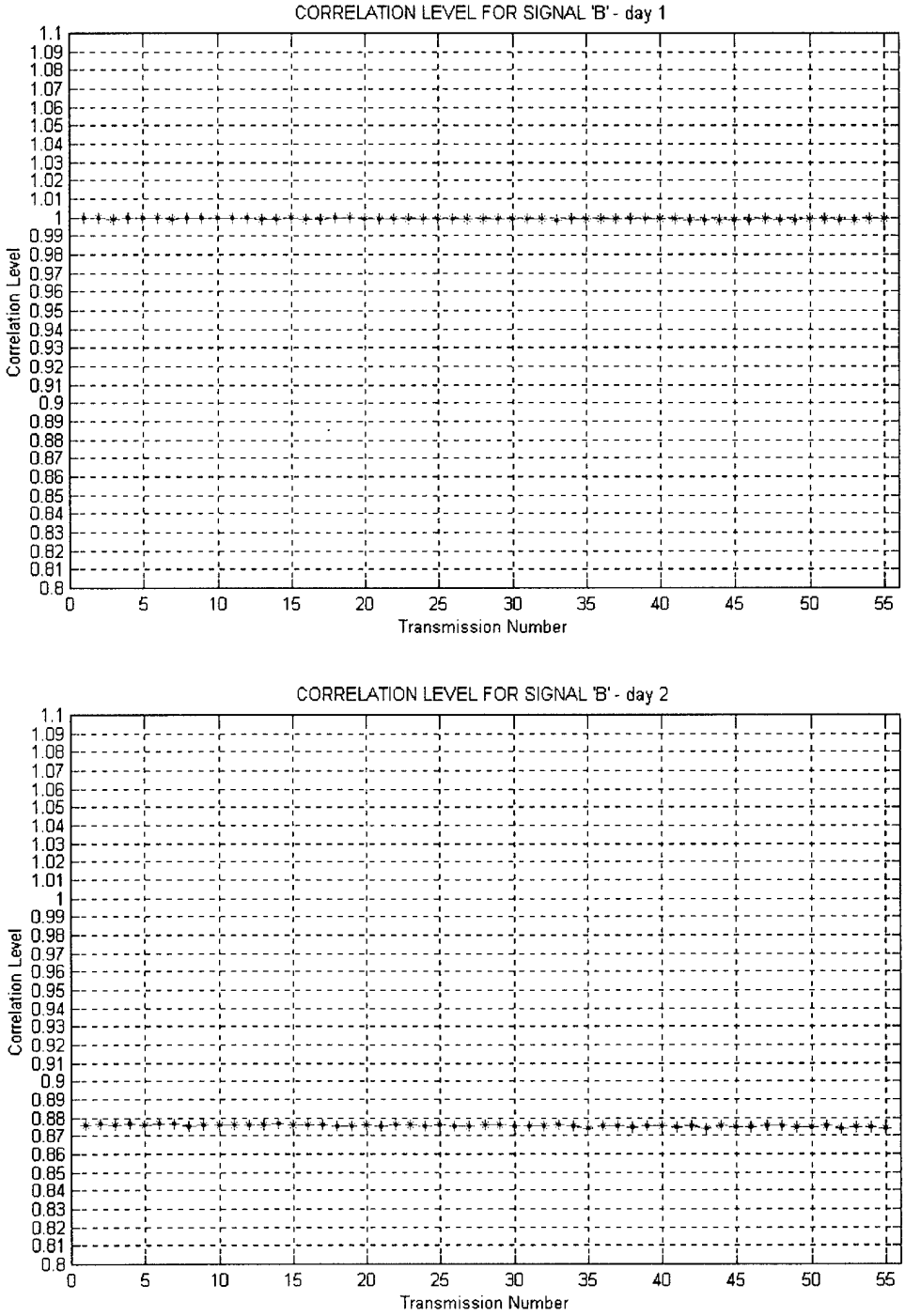

Figure 5.1b. Correlation Level for Signal B (Both days).

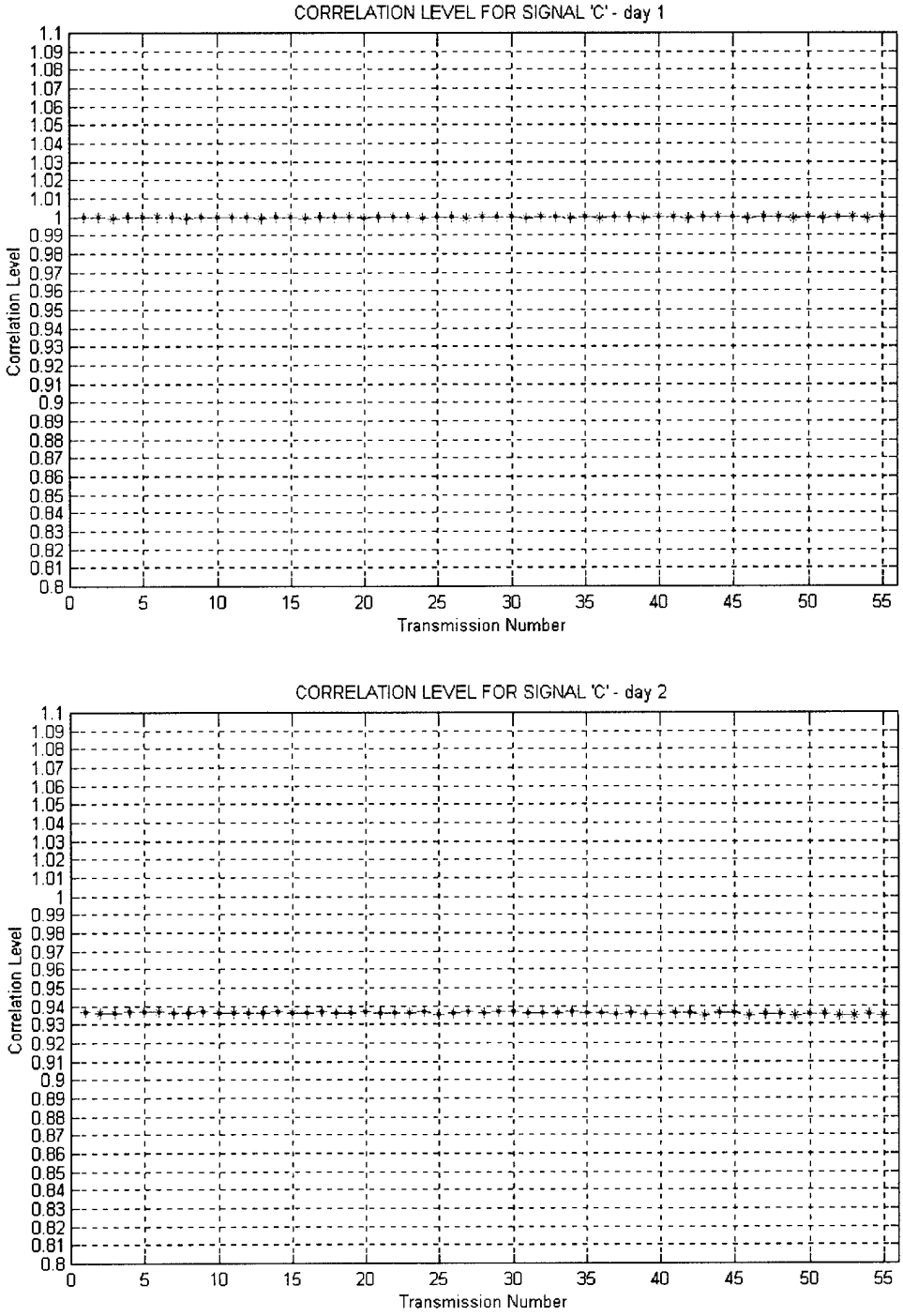

Figure 5.1c. Correlation Level for Signal C (Both days).

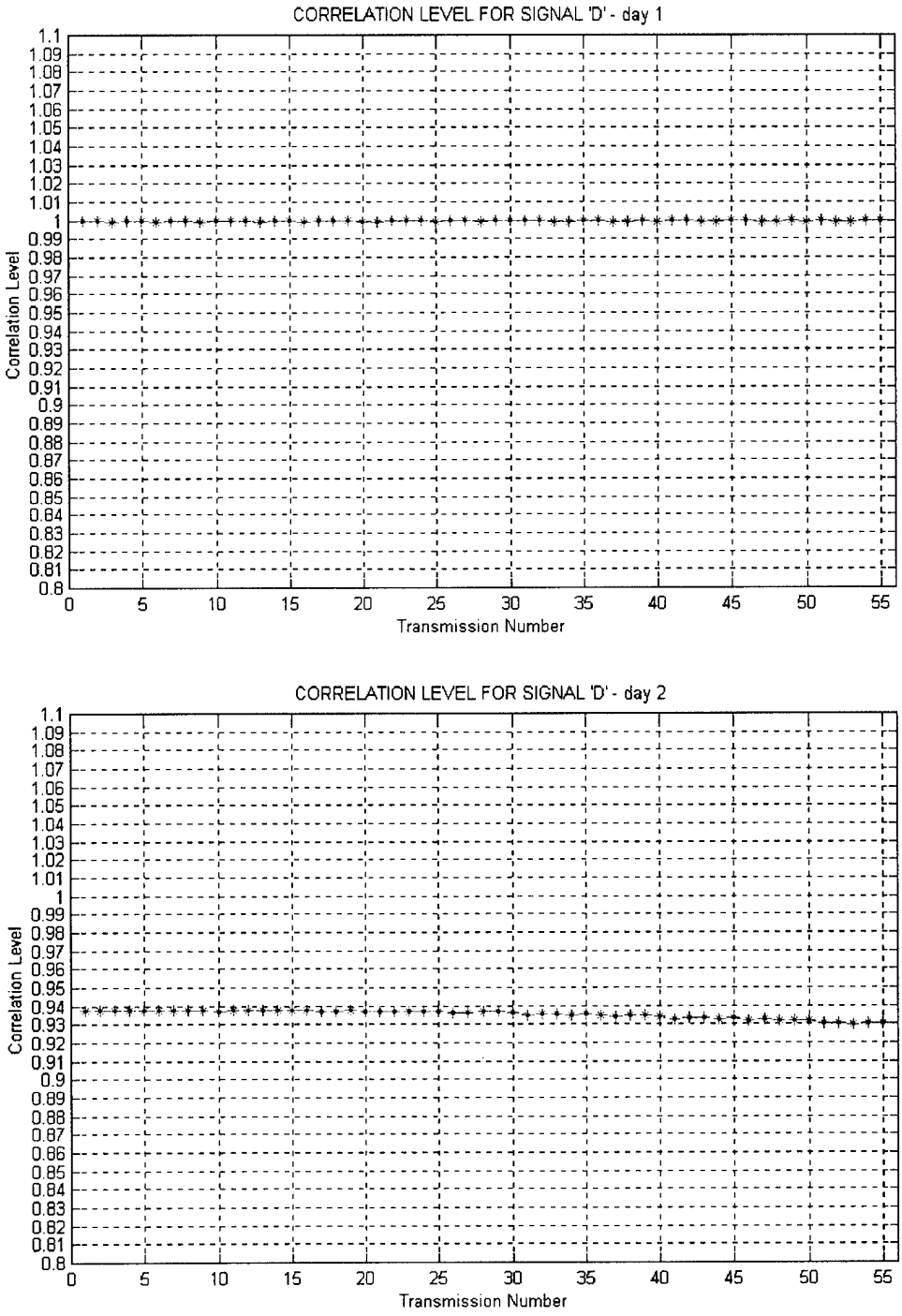

Figure 5.1d. Correlation Level for Signal D (Both days).

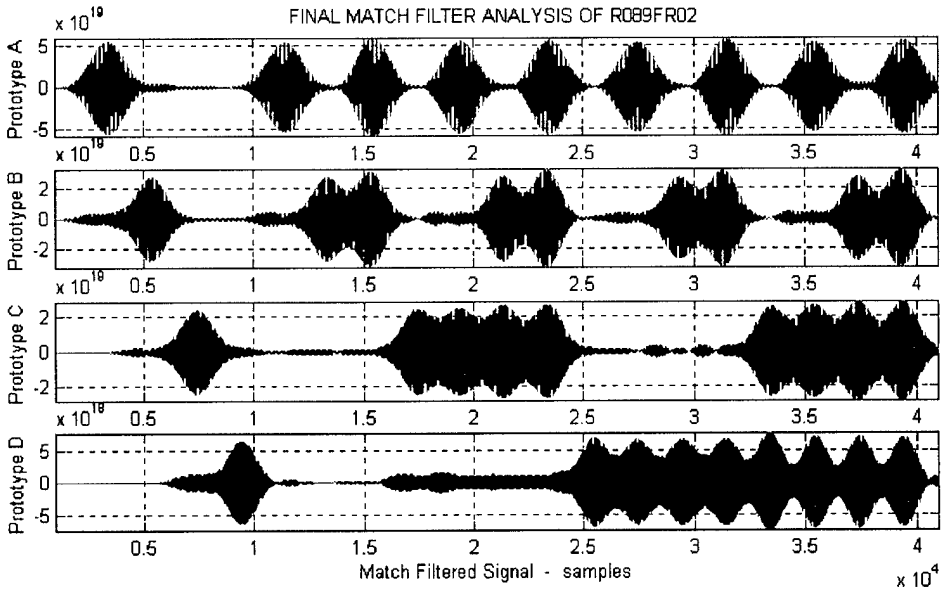

Figure 5.2. Message Resolved Using Prototypes Captured the Previous Day.

This change in the correlation level can be attributed to temperature difference between days and decrease of the water level due to evaporation. For the rest of the tests conducted, prototypes captured the same day with the message, were used for the processing.

B. SYMBOL RATE

The most important factors that determine the symbol rate used in a communication scheme are the center frequency spacing, the inter-symbol spacing and pulse width. The frequency spacing determines the resolution of the information contained within the symbol. In our experiment, the frequency spacing has been kept constant and is the same as that used by Heinemann (2000). The inter-symbol spacing is directly connected with the symbol rate and

its value is dictated by the ability to resolve the message using a communication scheme. The pulse length determines the bandwidth of the signal, and is indirectly related to false detection of a certain frequency component due to cross-talk between bits (frequencies).

1. Inter-Symbol Spacing Influence

We tried messages with symbol transmission intervals equal to 10, 5, 2, 1, and 0.4 ms (no spacing) and checked the ability to resolve the message. The results of our tests for inter-symbol spacing equal to 0.6 ms and 0 ms are shown in Fig. 5.3 and Fig. 5.4, respectively. We notice that even with no spacing between symbols the message is easily resolvable. Also, the level of cross-talk between bits (frequencies) is minimized and varies from 1/10 to ¼ of a received pulse peak after performing proccessing in the null-to-null bit bandwidth at a given center frequency. Also, the bits at 55 and 60 kHz suffer more than those at 50 and 65 kHz since at 55 and 60 kHz there is spectral overlap from two adjacent bits (frequencies on either side) whereas at 50 and 65 kHz there is spectral overlap from only one adjacent bit. In the first stage processing, where we match filter with signals A, B, C, and D, the cross-talk between bits (frequencies) is 2 times the previous value. We also tested the ability of the technique to resolve the message at different times and in the presence of many multipaths. In all cases the message was easily resolvable.

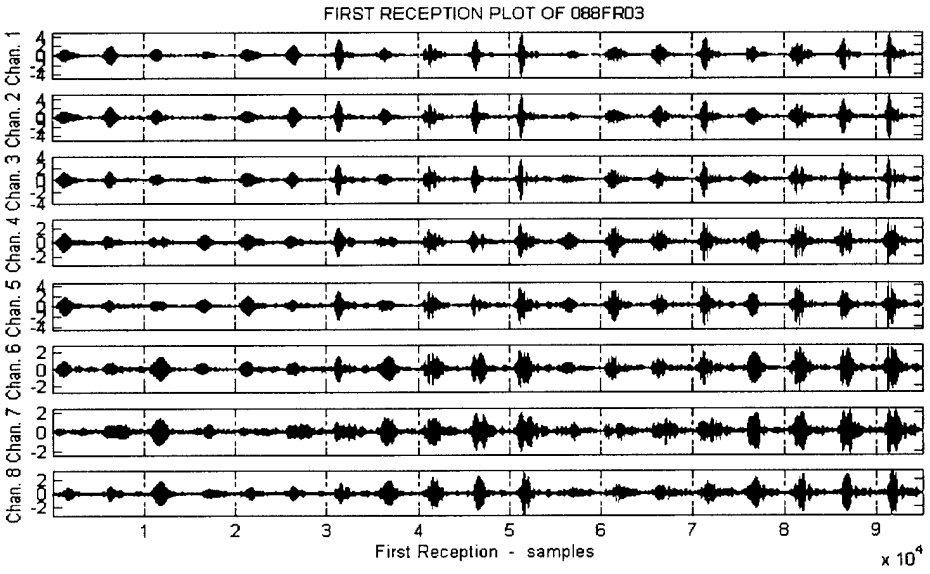

Figure 5.3a. First Reception of All Eight Channels Using 1 ms Spacing.

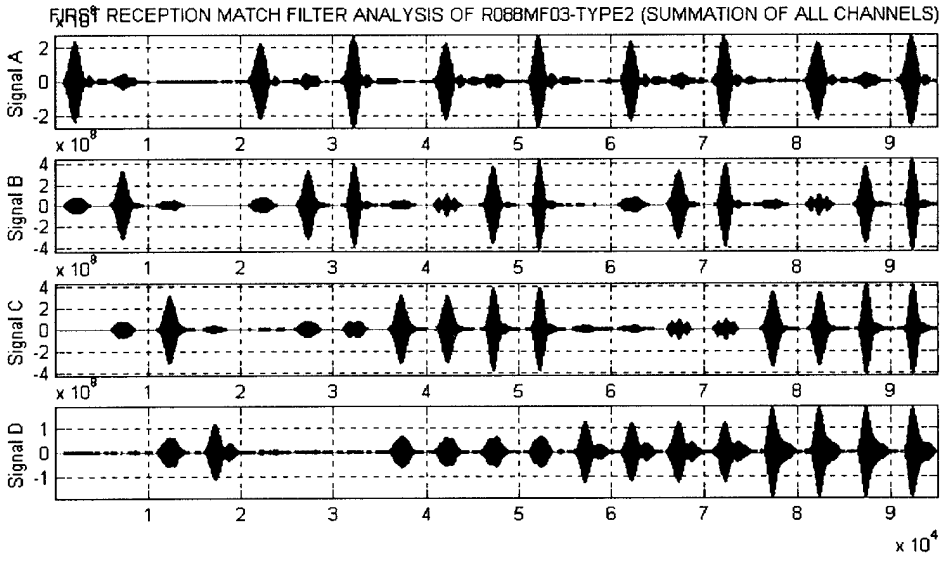

Figure 5.3b. First Stage Processing Output and Non-Coherent Summation of All Channels.

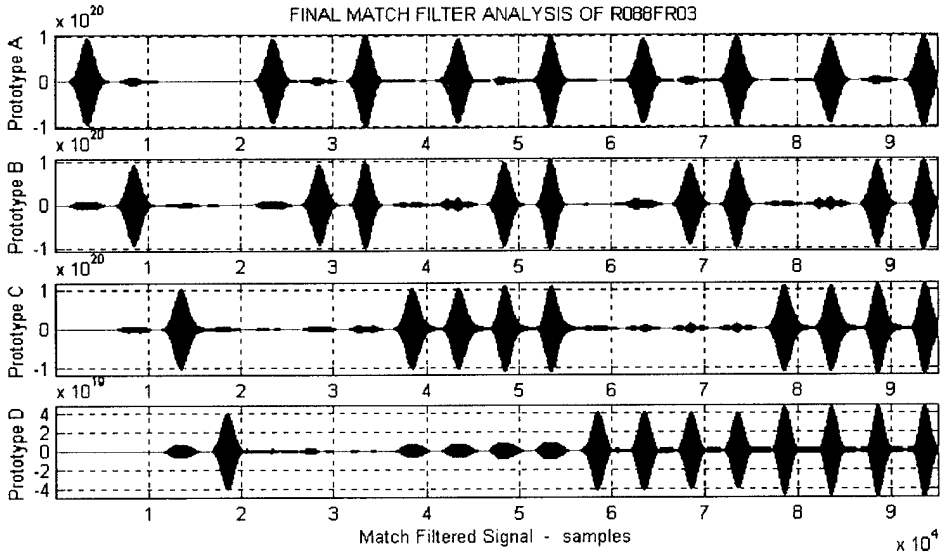

Figure 5.3c. Resolved Message after the Second Stage Processing.

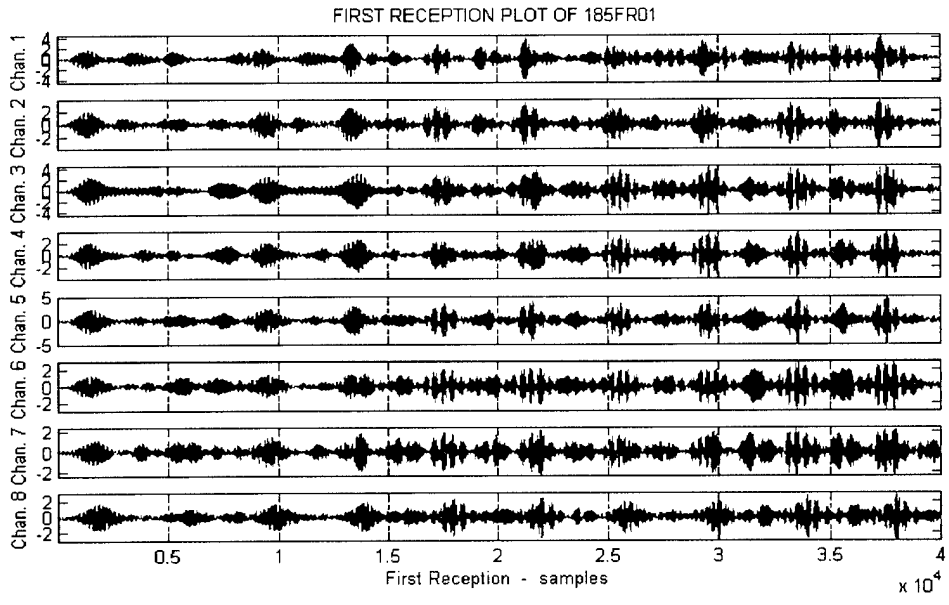

Figure 5.4a. First Reception of All Eight Channels Using 0.4 ms Spacing (no inter-symbol interval).

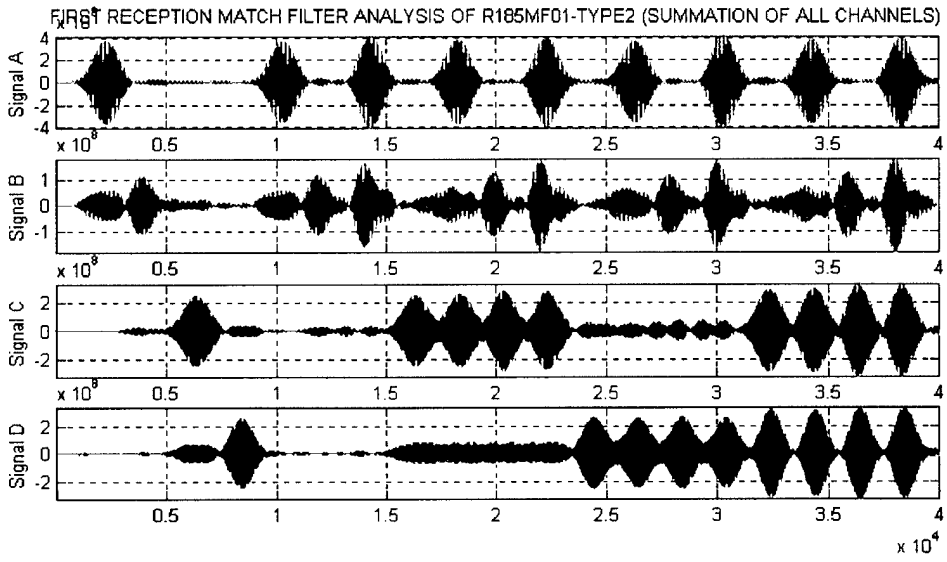

Figure 5.4b. First Stage Processing Output and Non-Coherent Summation of All Channels.

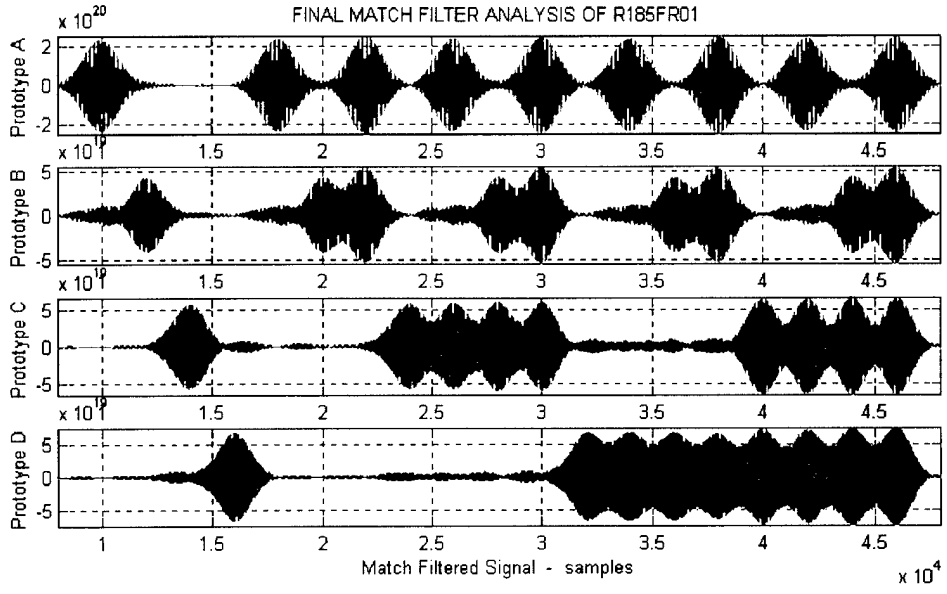

Figure 5.4c. Resolved Message after the Second Stage Processing.

We transmitted the same message using the TRAC approach. For this transmission, we used 1.6 ms, 0.6 ms, and no inter-symbol spacing, pulse length equal to 0.4 ms and Hanning window. The last two characteristics according to Heinemann (2000), is the best choice for the TRA approach. The message was synthesized using time-reversed receptions of 2 ms time span. The results are shown in Fig. 5.5.

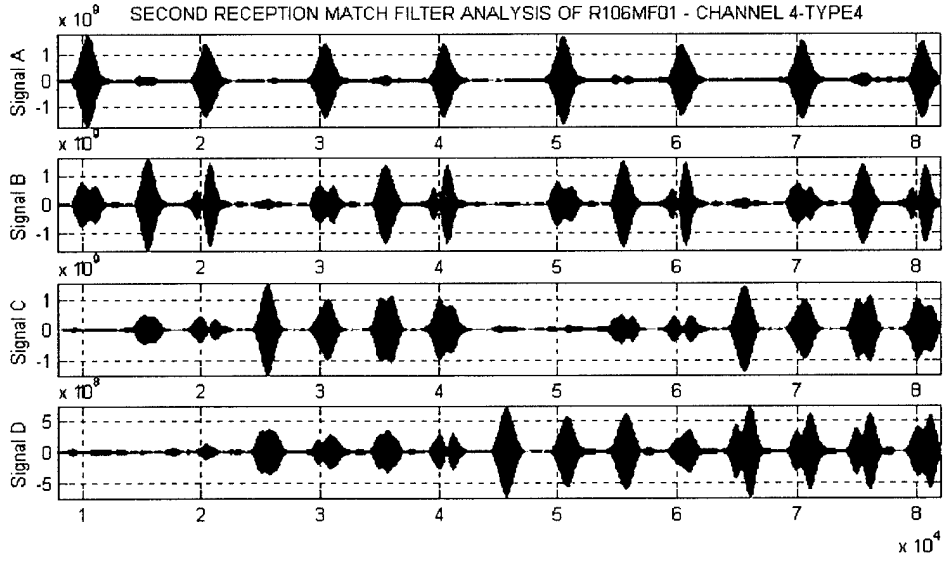

Figure 5.5a. Resolved Message after the TRA Processing (symbol spacing 1 ms).

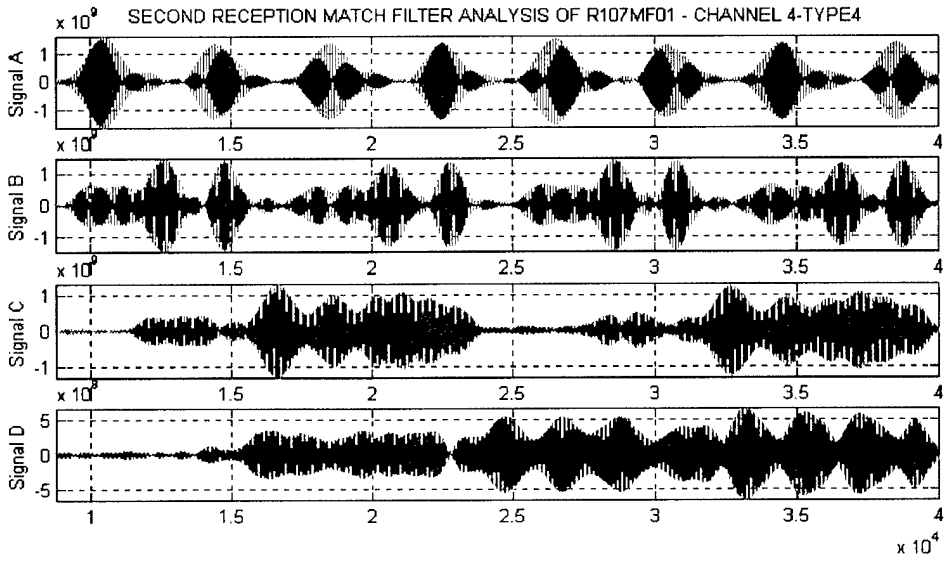

Figure 5.5b. Resolved Message after the TRA Processing (symbol spacing 0.4 ms).

We notice that using this method, the amplitude of the cross-talk between bits (frequencies) is equal to half of the amplitude of the main peak. This is much higher than the cross-talk amplitude using the MESS approach. Moreover, a splitting of the peak in the frequency of 60 kHz was observed. The most possible explanation for this is that the relative position of the time windows of 2 ms was not the same for all time-reversed signals of different frequencies. This created incorrect focusing in range for the unaligned frequency, an effect which also was observed while using the MESS approach during range-dependence resolution experiments. Finally, after transmitting messages using the TRA approach we noticed that the correlation level is not stable for different resolved symbols of the same message.

2. Transmitted Pulse Length Influence

We used a pulse length of ~0.29 ms, which corresponds to a null-to-null bit bandwidth equal to 14 kHz, in order to determine if the message was still resolvable. During this test, we maintained no guard time between transmitted symbols and we kept the center-frequency spacing the same as in previous tests. As a criterion for accepting a message as resolvable, we require that the side lobes (amplitude of cross-talk between bits (frequencies)) be less than half the amplitude of the main peaks. The results of our test are shown in Fig. 5.6. We notice that the message is still resolvable even if we use a shorter pulse for the symbols, while succeeding a symbol rate of 3500 symbols/sec.

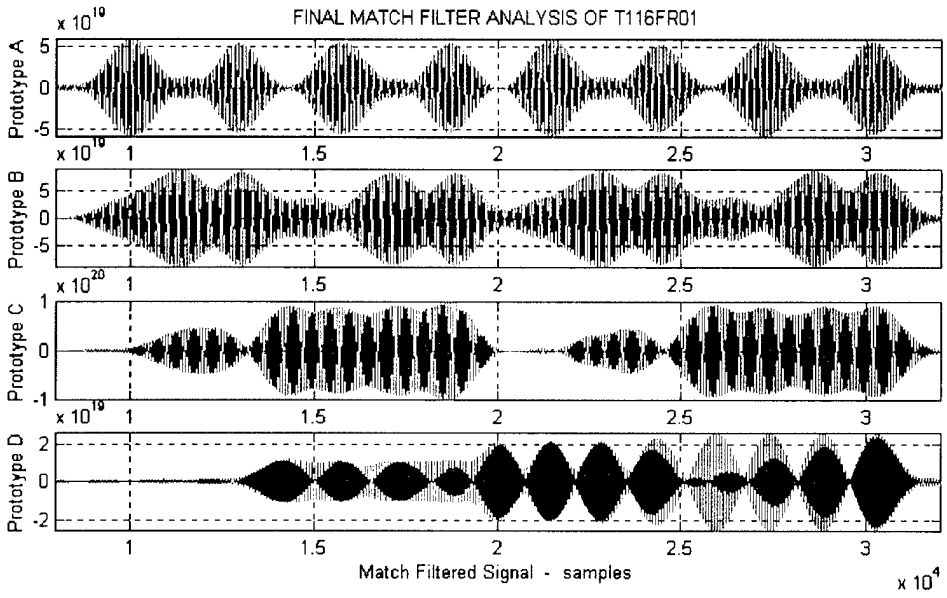

Figure 5.6. Resolved Message with Symbol Rate 3500 symbols/sec after Processed with MESS Technique (pulse length ~0.29 ms and no inter-symbol spacing).

Finally, we also tried to decrease the transmitted pulse length to 0.2 ms, which would give us a higher symbol rate (5000 symbols/sec). Using this pulse length the message becomes unresolvable due to high cross-talk amplitude between bits (frequencies).

C. RECEIVED PROBE SIGNAL LENGTH

We examined the resolvability of the message using the same reception but with received probe signals of different time span. In other words, we tried to find the minimum length of the received probe signals, used during the second stage match filtering, that allows us to resolve the message. During this test, we kept the symbol rate equal to 2500 symbols/sec and the transmitted pulse length equal to 0.4 ms with no guuard times between symbols. Also, we used received probe signal records of 0.4, 1, and 2 ms length. The results are shown in Fig. 5.7, where the received probe signal is referred to as prototype signal . The message is not resolvable for a time span equal to 0.4 ms, presenting very high cross-talk amplitude between bits and unstable correlation level for real peaks, which can lead to false interpretation of the message. The message is resolvable for the other two lengths. For probe signal records equal to 2 ms the cross-talk amplitude is higher than the 1 ms case but the resolution of the symbols increases. For all the processing done in the experiments, probe signal records of 2 ms length were used.

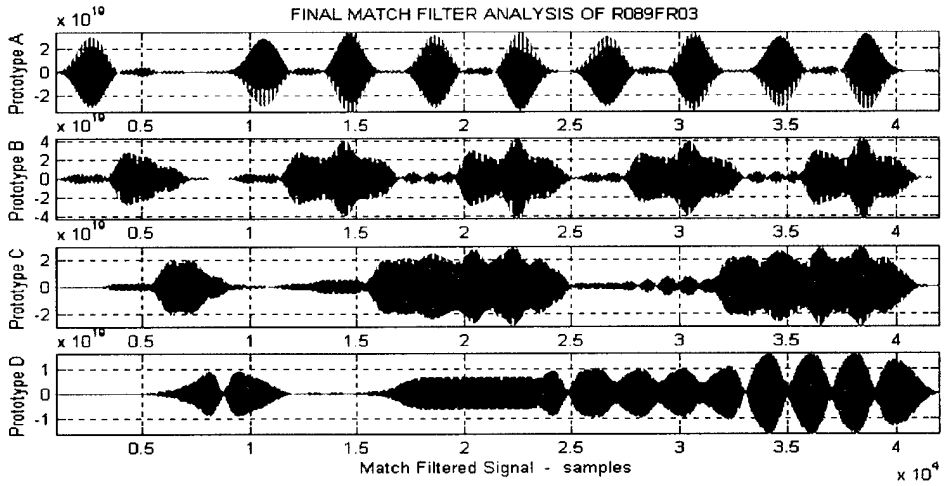

Figure 5.7a. Unresolvable Message after MESS Processing (underwater channel transfer function length 0.4 ms used in processing).

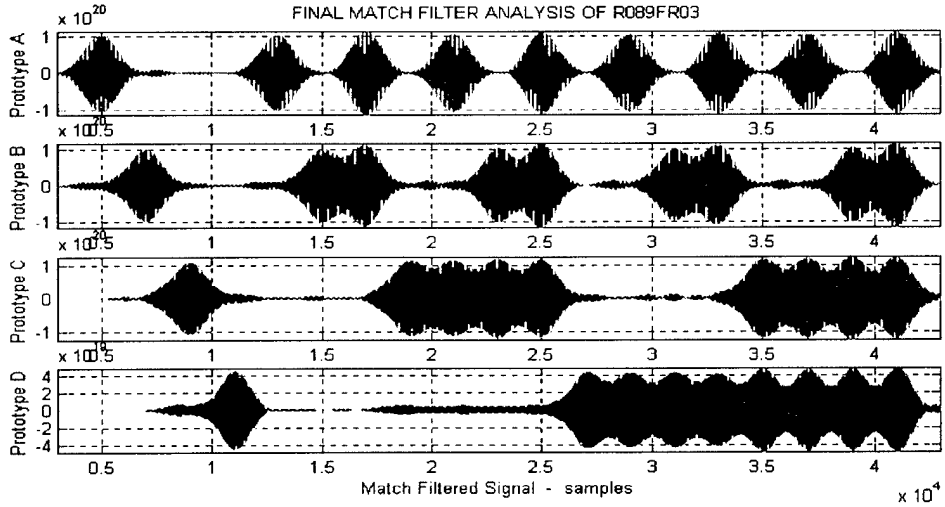

Figure 5.7b. Resolvable Message with Very Low Cross-talk Level after MESS Processing (underwater channel transfer length 1 ms used in processing).

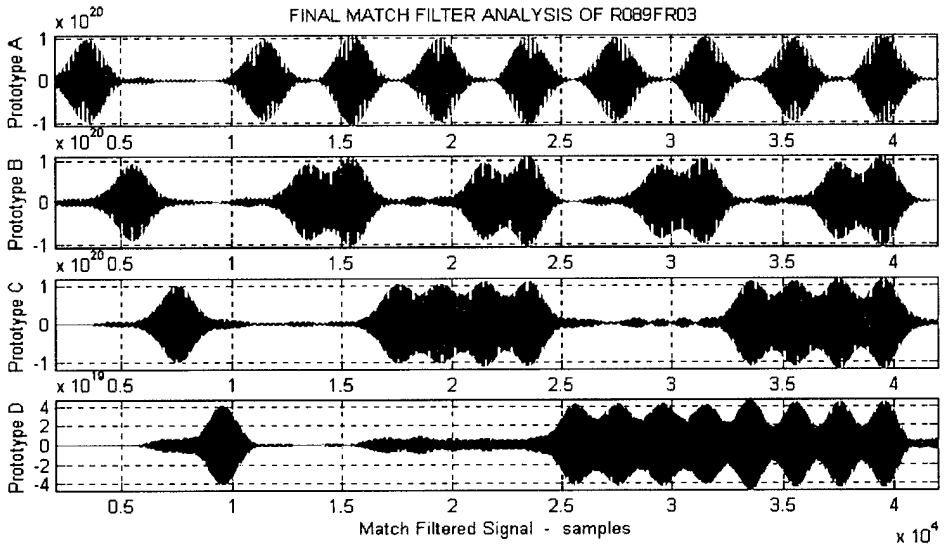

Figure 5.7c. Message with Improved Resolution of Symbols after MESS Processing (underwater channel transfer function length 2 ms used in processing)

D. SURFACE WAVE PRESENCE INFLUENCE

We investigated the influence of surface waves on the correlation level for each frequency used. In Fig. 5.7a through Fig.5.7d, where the correlation level is plotted for both cases, with and without surface waves and for all frequencies, we notice that surface waves do not alter the transfer function of the channel for our in-lab environment. Only for the case of signal D (center frequency 65 kHz) did we observe a decrease of the order of 10% in the correlation level, which does not drastically affect the resolution of the message.

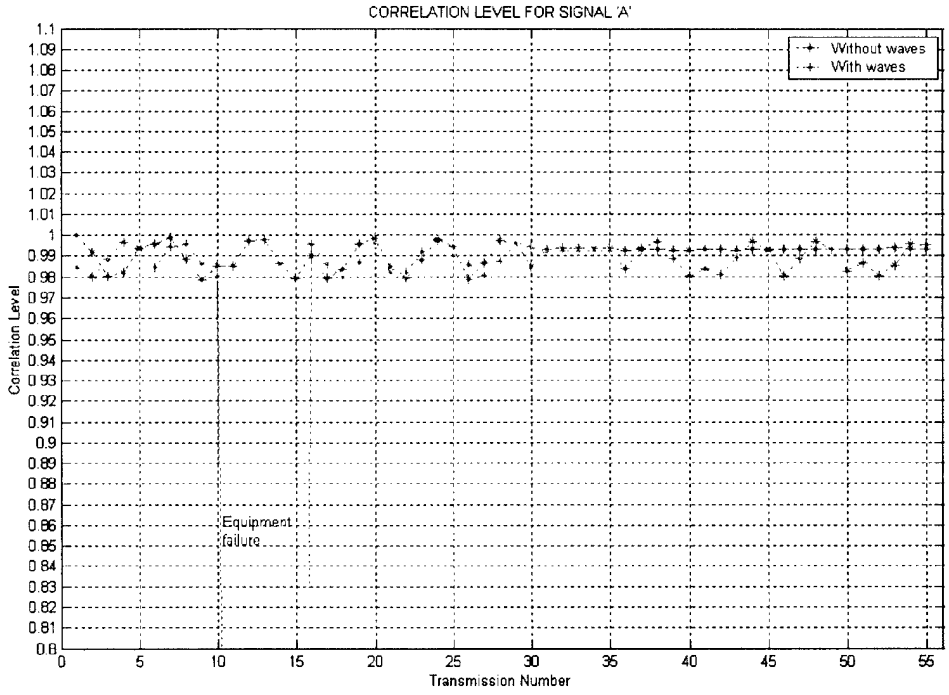

Figure 5.7a. Influence of Surface Waves on the Correlation Level for Signal A.

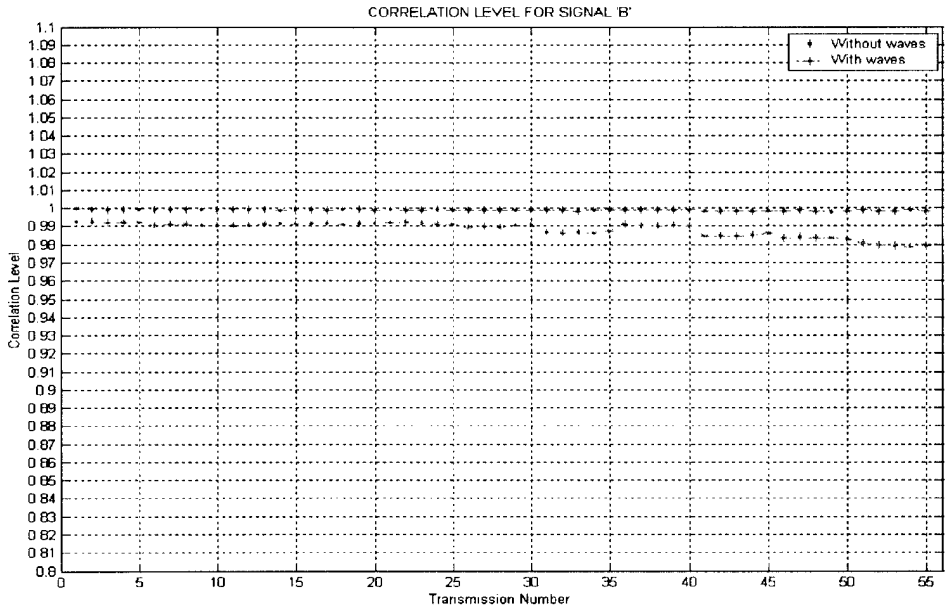

Figure 5.7b. Influence of Surface Waves on the Correlation Level for Signal B.

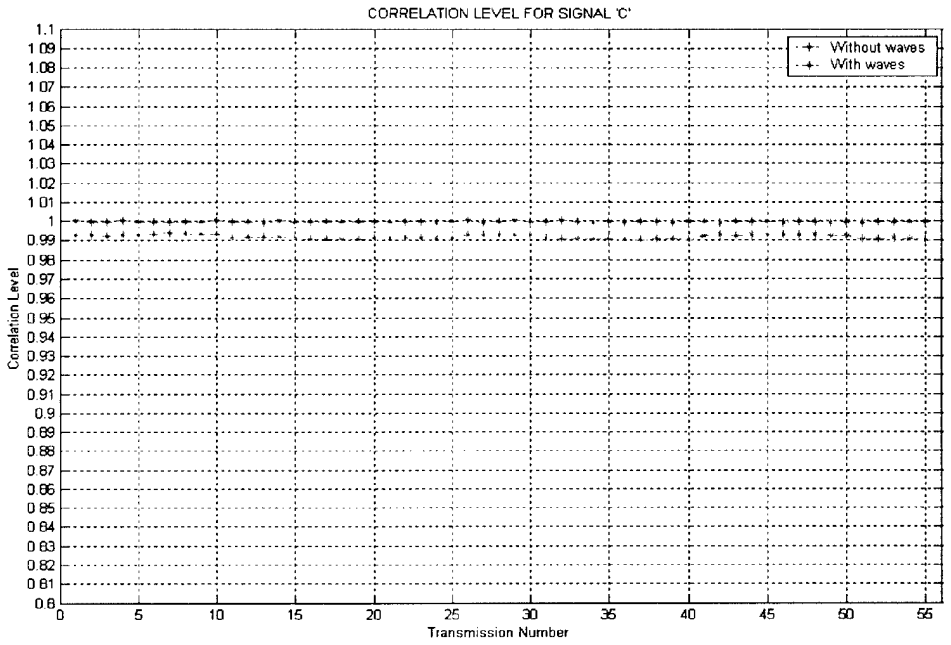

Figure 5.7c. Influence of Surface Waves on the Correlation Level for Signal C.

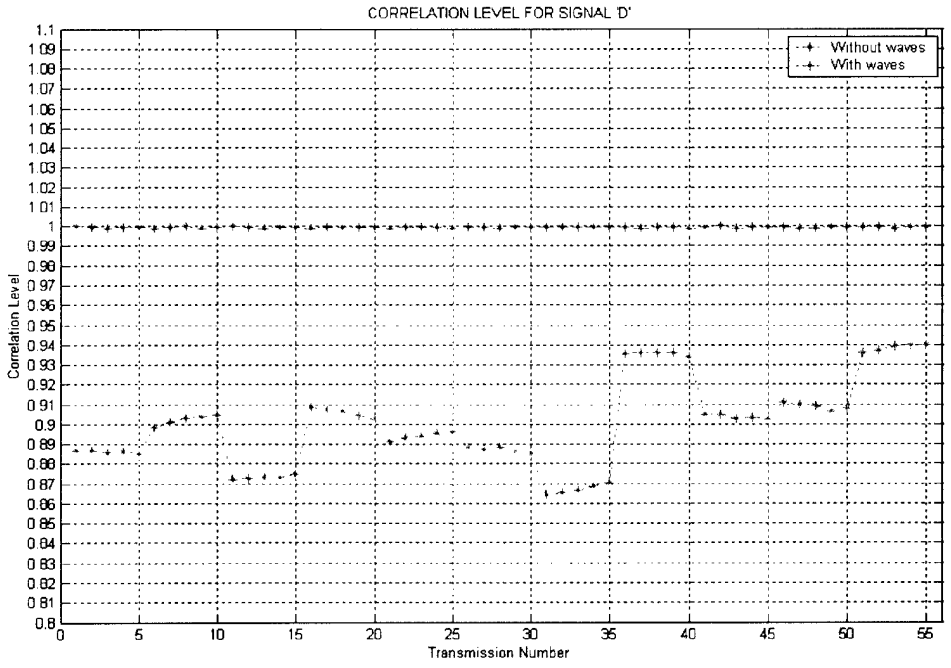

Figure 5.7d. Influence of Surface Waves on the Correlation Level for Signal D.

For validation of these results, that is, the weak influence of surface waves on the correlation level, we created surface waves with wavelength 2.3 cm (worst case scenario), transmitted a message, and processed the reception using the MESS approach. We notice that the message is easily resolvable (Fig. 5.8).

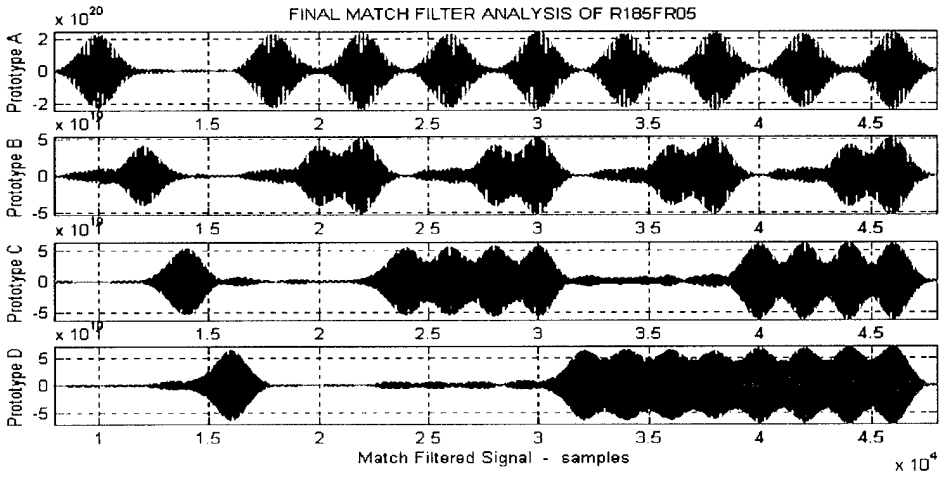

Figure 5.8. Influence of Surface Waves on Message Resolvability (surface waves of 2.3 cm wavelength present).

E. RANGE DEPENDENCY

We investigated the resolvability of the message for different ranges from the position where we captured the prototypes for the MESS approach. The same test, with the time-reversed receptions captured at different distances than the messages were, was conducted using the TRAC approach. We noticed that the MESS approach is very robust and let us resolve the message even if we set the distance between the arrays a half meter greater than the original, which is 20 times the average wavelength used. We also observed that when closing the distance between source and receiver, the message becomes unresolvable

much quicker than when opening the distance. This can be attributed to the fact that more modes are present at distances shorter than the initial, where the prototype was acquired. These modes alter the transfer function of the underwater channel and as a result there is not perfect matching between the prototypes and the message. At greater distances, these modes have been attenuated enough in order not to contribute to the transfer function. In this case, the message becomes unresolvable when the modes present at the initial distance begin to attenuate considerably. The results of this test are shown in Fig. 5.9. The tests performed at the distance of 5 m also verified the above observations.

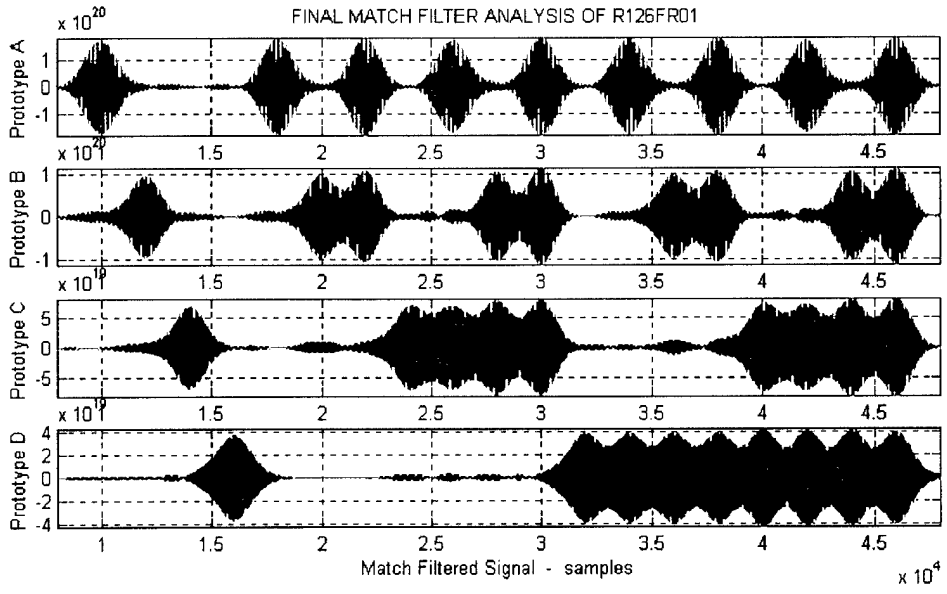

Figure 5.9a. Resolved Message at 4 m Using MESS Approach.

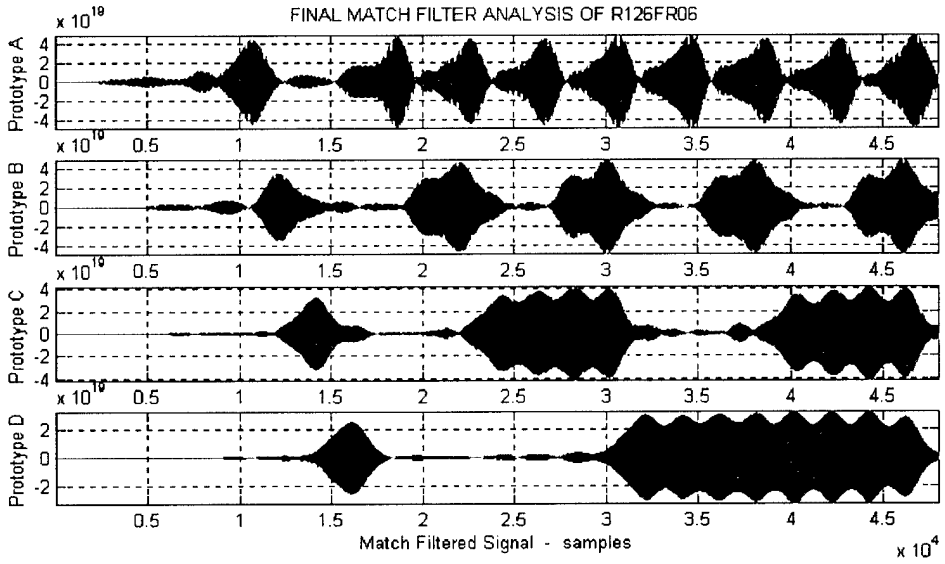

Figure 5.9b. Resolved Message at 4 m +50 cm Using MESS Approach.

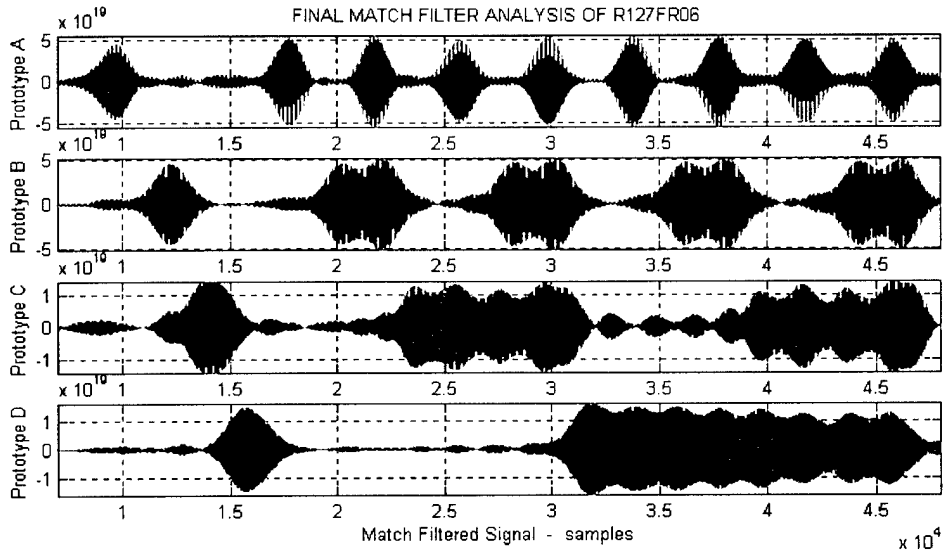

Figure 5.9c. Resolved Message at 4 m -50 cm Using MESS Approach. Notice the correlation level fluctuations at 60 and 65 kHz (for signals C and D).

The same test was performed using the TRAC approach. The results, shown in Fig. 5.10, make clear that this scheme is very sensitive to range changes. Particularly, the maximum distance that the message can be resolved using this method, is +30 cm and –20 cm of the original. This corresponds to + 12 times the average wavelength when increasing the distance and – 8 times the average wavelength when decreasing the distance. This sensitivity to range provides a message processed using TRAC scheme with natural encryption. However, small changes in range between the arrays can render the message unresolvable.

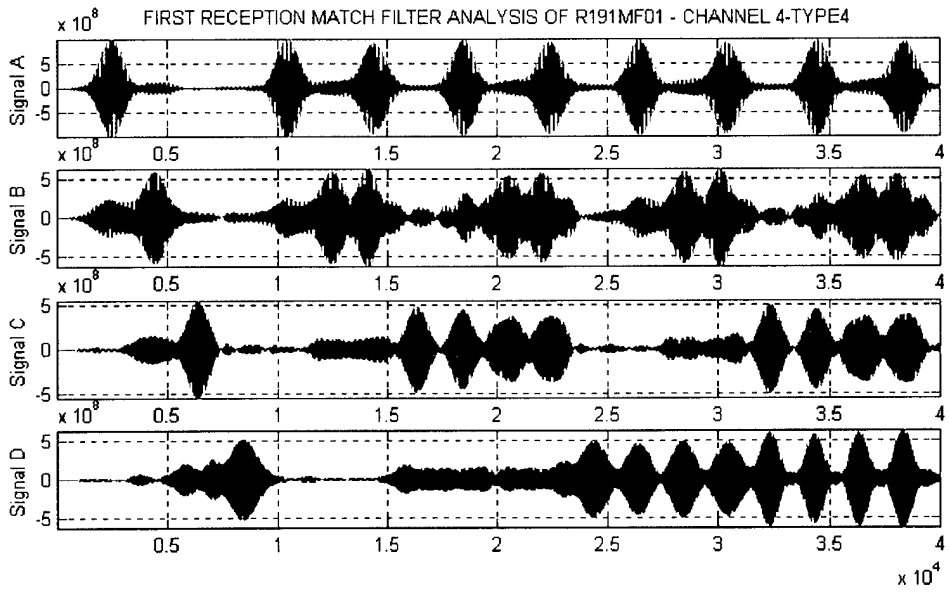

Figure 5.10a. Resolved Message at Focus Location Using TRAC Approach (channel 4 at range of 4 m).

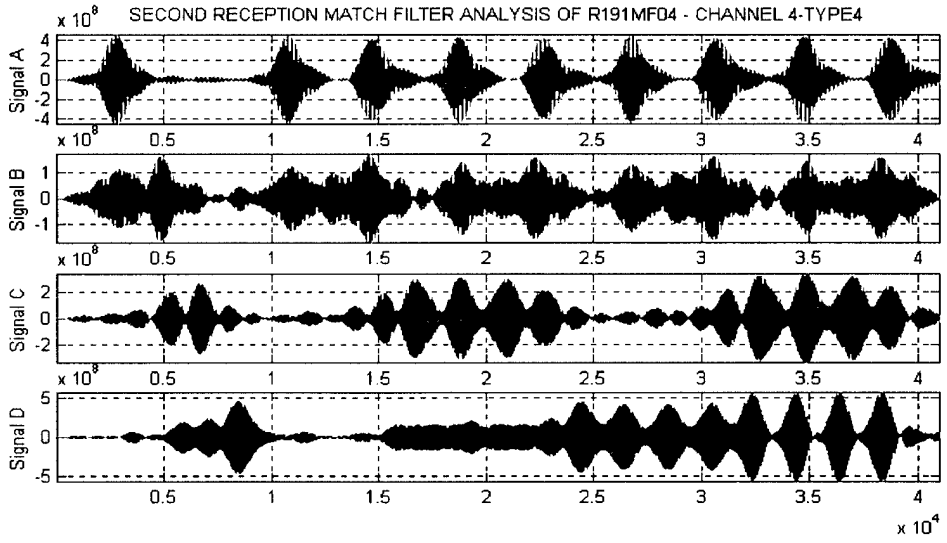

Figure 5.10b. Unresolvable Message Using TRAC Approach at 4 m + 30 cm (frequency 55 kHz , signal B, not resolved).

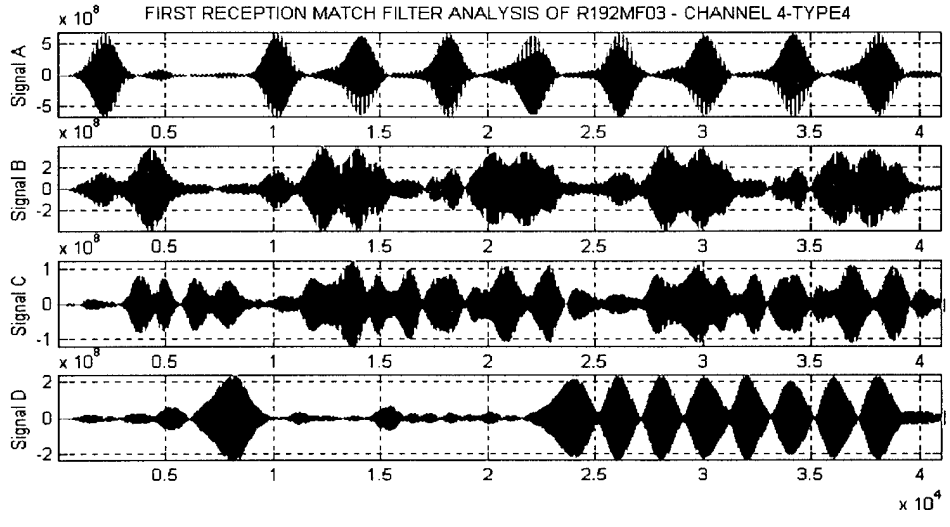

Figure 5.10c. Unresolvable Message Using TRAC Approach at 4 m - 20 cm off Focus Location (frequency 60 kHz, signal C, not resolved).

F. NOISE INFLUENCE

We investigated the robustness of the two methods for eight different noise levels. The SNR level for each signal A, B, C, and D was computed each time. The minimum SNR level for which the message is still resolvable was then determined. We noticed that the MESS approach is more robust than the TRAC approach, having better resolution at very low SNR's.

Specifically, for the MESS approach, the message is unresolvable for values below SNR_A= -1.8 dB, SNR_B= 3.4 dB, SNR_C= 0.8 dB, and SNR_D= 1.4 dB. For the TRAC approach, the message can be resolved for values equal or larger than SNR_A=8.8 dB, SNR_B= 4.5 dB, SNR_C=10.5 dB, and SNR_D=7.4 dB. The SNR improvement we get using the MESS method can be attributed to the fact that not only the message but also the time-reversed signals, used for the message creation in the TRAC aproach, already contain noise, since they are transmitted through the noisy channel. As a result, the noise power is much greater in the TRAC method than in the MESS approach. The difference in SNR's between frequencies can be justified by the fact that the transfer function of the receiver-transmitter varies with respect to frequency. Also, due to randomness of noise in the selected band the power spectral density is not constant, and as a result the SNR is different between frequencies. The results from the MESS and the TRAC approaches for the marginal values of SNR's are shown in Fig. 5.11 and 5.12, respectively. These figures present the cases in which the message could not be resolved for at least one frequency.

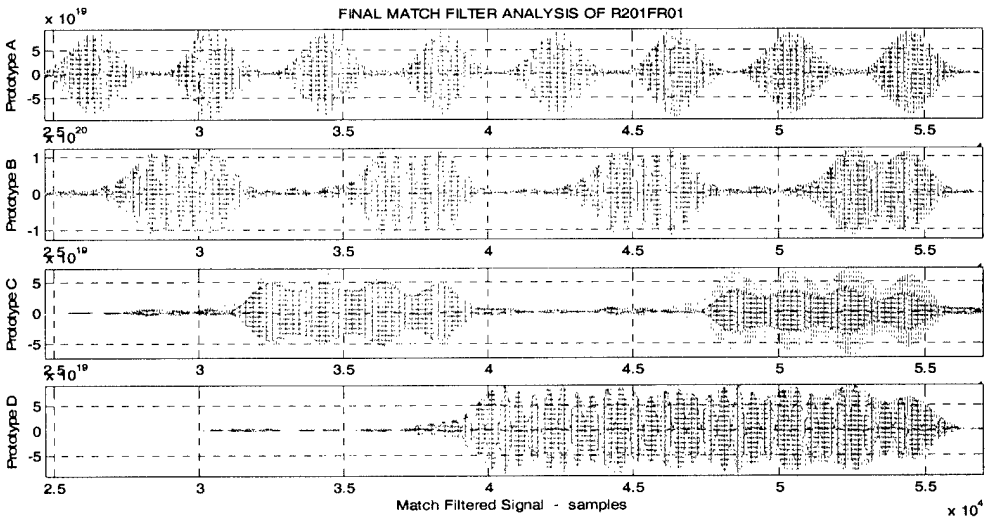

Figure 5.11a. Resolvable Message Using MESS Approach Transmitted in a Non-Noisy Environment.

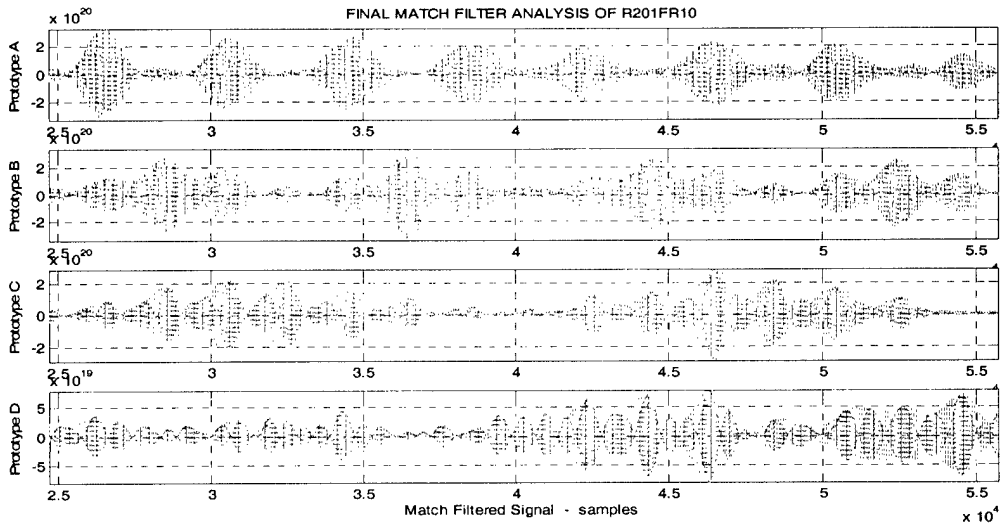

Figure 5.11b. Unresolvable Message Using MESS Approach Transmitted in a Noisy Environment (SNR_A= -1.8 dB, SNR_B= 3.4 dB, SNR_C= 0.8 dB, and SNR_D= 1.4 dB).

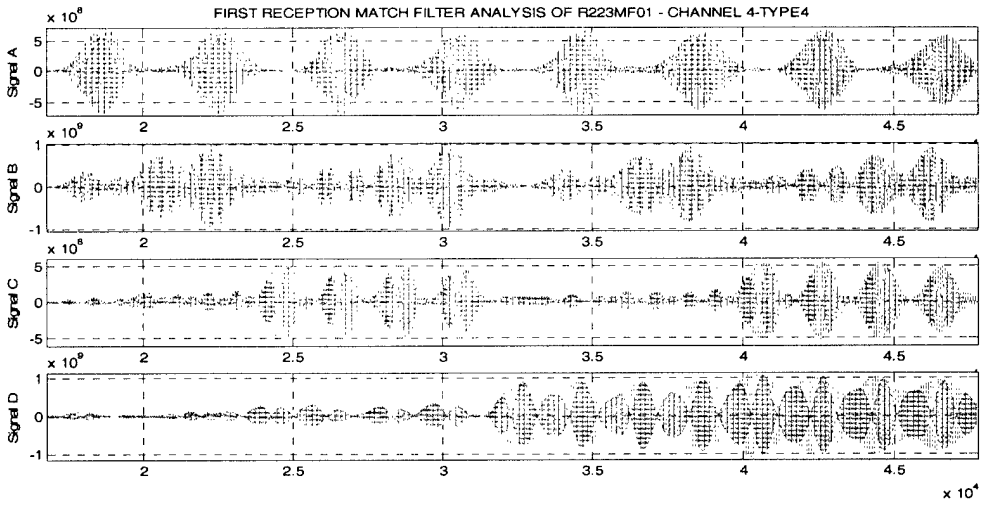

Figure 5.12a. Resolvable Message Using TRAC Approach Transmitted in a Non-Noisy Environment.

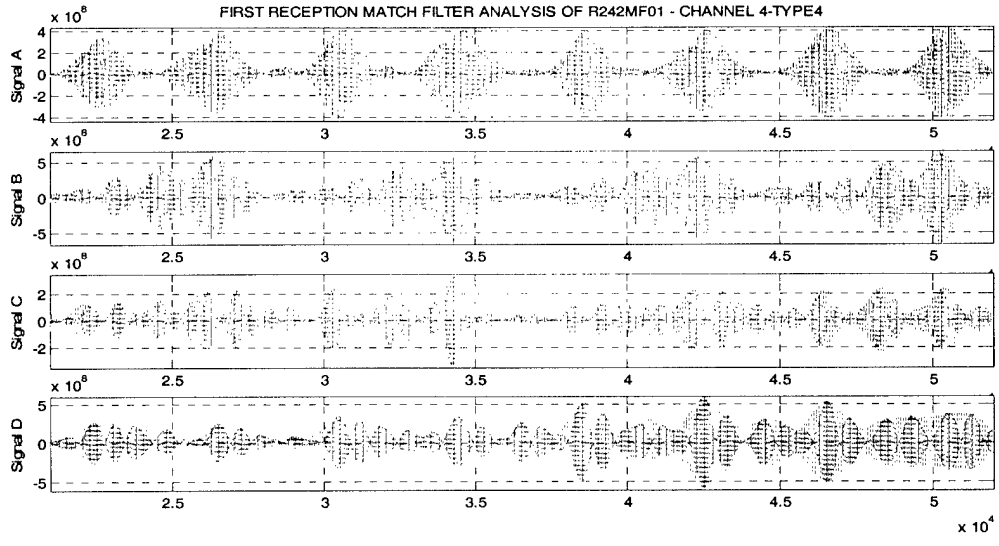

Figure 5.12b. Resolvable Message Using TRAC Approach Transmitted in a Noisy Environment (SNR_A=13.6 dB, SNR_B=17 dB, SNR_C=10.5 dB, and SNR_D=7.4 dB).

VI. CONCLUSIONS

A. METHODS COMPARISON

We conducted experimental studies and data analysis to investigate the robustness of the MESS method and compared it with the TRAC approach. Experimental results indicate a good basis for further experimental work on the MESS approach, both for in-lab experiments and at-sea underwater trials.

We investigated the robustness of the MESS method with respect to time and under the influence of surface waves. Results show that correlation levels remain almost unchanged during the same day and decrease the following day with such rate that allows us to resolve a message using received probe signals captured the previous day. Results also indicate surface waves have little or no effect on correlation levels, allowing the message to be resolved without difficulty. However, the unaffected correlation due to surface waves can be explained by noticing that the waves were generated with conical pistons whose size is comparable with the wavelength of the waves, leading to cylindrical spreading and localized wave excitation regions. The scattering of sound by the rough surface and the Doppler effects were thus minimized, leaving the correlation level unaffected.

The computational load in the MESS method is very heavy, demanding fast processors and a large memory size due to the two correlation computations performed. Note that this load could be significantly decreased by using an FFT approach, where a power of 2 is selected in the computations. That is, compute

the FFT of the message and the signals to be matched, multiply the first with the conjugate of the second, then compute the IFFT of the product.

The TRAC method has less computational complexity, as the underwater channel acts as the matched filter. However, the TRAC approach requires more power for transmission than the MESS approach, as all eight channels are used for transmission.

Experiments indicate that a symbol rate of 2500 symbols/sec is guaranteed for both methods when using a center-frequency spacing of 5 kHz, pulse length equal to 0.4 ms, and no inter-symbol spacing, which corresponds to a 10000 bits/sec data rate. These characteristics give us a spectral efficiency of (4 b/.4 ms)/25 kHz = 0.4 b/s/Hz for our basic signal. The MESS approach shows very low cross-talk amplitude between bits (frequencies), which ranges between ¼ - ½ of the cross-talk amplitude measured in the TRAC approach. Symbols resolution is improved and well-shaped pulses are created after processing the reception with the MESS approach. In addition, "peak splitting" using the TRAC method is very difficult to avoid, due to the sensitivity of the technique to the selection of the same time window for time-reversed signals.

We also investigated the ability of the MESS method to provide a higher data rate than the maximum rate the TRAC method provides, while keeping the cross-talk amplitude at less than the half of the maximum amplitude of the real peak. For this purpose, we decreased the pulse length to ~0.29 ms, which corresponded to a symbol rate of 3500 symbols/sec. Experimental tests showed

that it is feasible to achieve this data rate while maintaining the ability to resolve the message.

Experiments also show that the MESS approach is more robust in range changes than the TRAC approach. Specifically, we were able to resolve the message even 20 wavelengths away from the position where the replica of the transfer function of the channel was captured. The TRAC method proved to be very sensitive to range changes, as the absence of time focusing causes intersymbol interference outside the focal region. However, this sensitivity attributes a natural encryption to the message transmitted using the TRAC method for points outside the focal region.

Finally, we investigated the robustness of both methods in the presence of noise. For the evaluation of each scheme we computed the minimum SNR required for each center frequency in order for the message to be resolvable. The MESS approach displayed much better behavior in the presence of noise allowing us to resolve the message without errors for lower SNR's than the TRAC approach for all frequencies used. Specifically, using the MESS approach, we managed to resolve the message for SNR values approximately 1-10 dB less than those obtained by using the TRAC approach. The SNR improvement we get using the MESS method can be attributed to the fact that not only the message but also the time-reversed signals, used for the message creation in the TRAC aproach, already contain noise, since they are transmitted through the noisy channel. As a result, the noise power is much greater in the TRAC method than in the MESS approach.

B. RECOMMENDATIONS FOR FURTHER EXPERIMENTS

Experiments show that the influence of surface waves on the correlation level and the ability to resolve the message should be investigated more thoroughly. Radial waves were created in our experiments to decay approximately proporsionally with 1/R, where R is the distance from the wave source. As a result, the surface waves that are created are of low intensity even if the wave generators are very close to the arrays. A possible solution would be to create planar waves of high intensity and investigate the robustness of the MESS approach in a drastically changing environment.

During our tests the MESS method demonstrated very good stability with respect to the correlation level. We could take advantage of this feature, utilize two or even three amplitude levels and create more symbols instead of using one amplitude level for each frequency. As a result, the data rate and consequently the bandwidth efficiency would increase significantly. In-tank experiments should also be conducted to verify the robustness of this modified signaling scheme. For these experiments the best choice for the signal design would be to use pulses of 0.4 ms duration, no inter-symbol spacing and a channel transfer function of 1 ms duration, as these characteristics result in low cross-talk level and high symbol rate. Note that the presence of more than one amplitude levels for the TRAC method is not recommended due to correlation level fluctuations observed during our tests.

Finally, the robustness of the MESS method should be further studied in realistic environments, which could be achieved by conducting further in-tank

experiments or performing tests under real underwater environment conditions during sea trials.

THIS PAGE INTENTIONALLY LEFT BLANK

LIST OF REFERENCES

Abrantes, A.A.M., Smith, K.B., and Larraza, A., **(1999)**, "Examination of Time-Reversal Acoustics and Applications to Underwater Communications," *Journal of the Acoustical Society of America*, Vol. 105, pp. 1364

EDO Corporation, Acoustic Division, **(1998)**, Calibration Reports Serial # 5815-001/002

Gage Applied Sciences Inc., **(1998)**, CompuGen 1100 - Hardware Manual and Installation Guide, 2nd Ed.

Gage Applied Sciences Inc., **(1998)**, CompuScope 512 - Hardware Manual and Installation Guide, 1st Ed.

Heinemann, M. G., **(2000)**, *Experimental Studies of Applications of Time-Reversal Acoustics to Non-coherent Underwater Communications, Master's Thesis,* Naval Postgraduate School, Monterey, Ca

Jensen, F.B., Kuperman, W.A., Porter, M.B., Schmidt, H., **(2000)**, *Computational Ocean Acoustics, American Institute of Physics*

Kilfoyle, D. B., Baggeroer, A. B., **(2000)**, "The State of Art in Underwater Acoustic Telemetry," *IEEE Journal of Oceanic Engineering,* Vol. 25, No. 1, pp. 4-27

Kuperman, W. A., Hodgkiss, W.S., Song, H.C., Akal, T., Ferla, C., Jackson, D.R., **(1998)**, "Phase Conjugation in the Ocean: Experimental Demonstration of an Acoustic Time-Reversal Mirror," *Journal of the Acoustical Society of America*, Vol. 103, Pt. 1, pp. 25-40

Proakis, J. G., Manolakis, D. G., **(1996)**, *Digital Signal Processing: Principal and Applications, Prentice Hall, Upper Saddle River, NJ*

Smith, K.B., Abrantes, A.A.M. and Larraza, A., **(1999)**, "Examination of time-reversal acosutics in shallow water and applications to noncoherent underwater acoustic communications," Submitted to the *Journal of the Acoustical Society of America*

Stojanovic,M.,**(1995),** "Underwater Acoustic Communications," *IEEE Electro International, Professional Program Proceedings,* pp. 435-440

Stojanovic,M.,**(1996),** "Recent Advances in High-speed Underwater Acoustic Communications," *IEEE Journal of Oceanic Engineering,* Vol. 21, No. 2, pp. 125-136

INITIAL DISTRIBUTION LIST

1. Defense Technical Information Center 2
   8725 John J. Kingman Road, Suite 0944
   Ft. Belvoir, VA 22060-6218

2. Dudley Knox Library 2
   Naval Postgraduate School
   411 Dyer Road
   Monterey, CA 93943-5101

3. Prof. K.B. Smith, Code PH/Sk 3
   Department of Physics
   Naval Postgraduate School
   Monterey, CA 93943-5117

4. Prof. A. Larraza, Code PH/La 3
   Department of Physics
   Naval Postgraduate School
   Monterey, CA 93943-5117

5. Prof. M. P. Fargues, Code EC/Fa 1
   Department of Electrical and Computer Engineering
   Naval Postgraduate School
   Monterey, CA 93943-5121

6. Prof. R. Cristi, Code EC/Cx 1
   Department of Electrical Engineering
   Naval Postgraduate School
   Monterey, CA 93943-5121

7. Prof. J.B. Knorr, Code EC 1
   Department of Electrical and Computer Engineering
   Naval Postgraduate School
   Monterey, CA 93943-5121

8. Prof. W.B. Maier, Code PH/Mw 1
   Department of Physics
   Naval Postgraduate School
   Monterey, CA 93943-5117

9. Engineering and Technology Curricular Office (Code 34).....1
Naval Postgraduate School
700 Dyer Road, Room 115
Monterey, CA 93943-5109

10. Lt Christos Athanasiou.....3
2 Dexamenis Str., P. Faliro
Athens, 17561
GREECE